

8-2014

Unsteady Viscous Cavity Flow Using Computational Fluid Dynamics

Chandramouli Vadlamudi

Follow this and additional works at: <https://commons.erau.edu/edt>



Part of the [Aerospace Engineering Commons](#)

Scholarly Commons Citation

Vadlamudi, Chandramouli, "Unsteady Viscous Cavity Flow Using Computational Fluid Dynamics" (2014).
Dissertations and Theses. 255.

<https://commons.erau.edu/edt/255>

This Thesis - Open Access is brought to you for free and open access by Scholarly Commons. It has been accepted for inclusion in Dissertations and Theses by an authorized administrator of Scholarly Commons. For more information, please contact commons@erau.edu.

UNSTEADY VISCOUS CAVITY FLOW USING COMPUTATIONAL FLUID DYNAMICS

By

CHANDRAMOULI VADLAMUDI

A Thesis Submitted to the College of Engineering, Department of Aerospace Engineering
for the partial fulfillment of the requirements of the degree of

Master of Science in Aerospace Engineering

Embry-Riddle Aeronautical University

Daytona Beach, Florida

August 2014

UNSTEADY VISCOUS CAVITY FLOW USING COMPUTATIONAL FLUID DYNAMICS

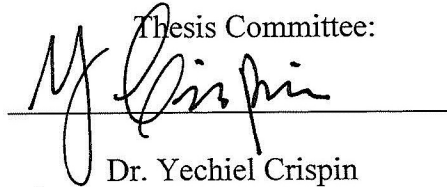
By

Chandramouli Vadlamudi

This thesis was prepared under the direction of the candidate's Thesis Committee Chair, Dr. Yechiel Crispin, Professor, Aerospace Engineering, Daytona Beach Campus, and Thesis Committee Members Dr. Reda Mankbadi, Professor, Aerospace Engineering, Daytona Beach Campus, and Dr. Dongeun Seo, Assistant Professor, Aerospace Engineering, Daytona Beach Campus, and has been approved by the Thesis Committee. It was submitted to the Department of Aerospace Engineering in partial fulfillment of the requirements for the degree of:

Master of Science in Aerospace Engineering

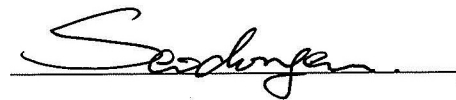
Thesis Committee:



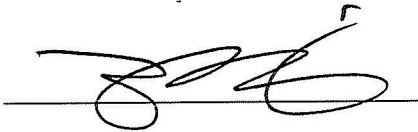
Dr. Yechiel Crispin
Committee Chair



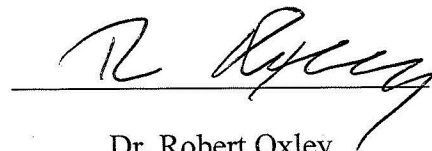
Dr. Reda Mankbadi
Committee Member



Dr. Dongeun Seo
Committee Member



Dr. Yi Zhao
Graduate Program Coordinator



Dr. Robert Oxley
Associate Vice President for Academics

Date: 9-26-14

ACKNOWLEDGEMENTS

I would like to express my sincere thanks to my advisor, Dr. Yechiel Crispin for his continuous support, suggestions and consistent encouragement. The completion of this thesis would have been impossible without his guidance.

I would like to express my sincere gratitude to the committee members, Dr. Reda Mankbadi and Dr. Dongeun Seo. I would also like to thank my friends who had helped me in the process of this thesis.

I cannot finish without expressing my deepest gratitude to my family and special friends for their continuous support, love, patience and encouragement during my academic years.

ABSTRACT

Author: Chandramouli Vadlamudi

Title: Unsteady Viscous Cavity Flow Using Computational Fluid Dynamics

Institution: Embry-Riddle Aeronautical University

Degree: Master of Science in Aerospace Engineering

Year: 2014

The problem of unsteady viscous incompressible flow in a two-dimensional cavity is treated using the unsteady incompressible Navier-Stokes equations with various initial and boundary conditions. First the case of a square cavity with one inlet and one outlet is treated in steady and unsteady flows. The software package ANSYS FLUENT was used in the CFD simulations. This approach captures the appearance of separation bubbles and vortex formation inside the cavity. Steady state flows are also obtained from the unsteady simulations after convergence of the time dependent solutions. Then the case of a cavity with a synthetic jet and two outlets is treated, where a complex configuration of vortices and bubbles form in the cavity.

TABLE OF CONTENTS

ACKNOWLEDGEMENTS	iii
ABSTRACT	iv
LIST OF FIGURES	viii
LIST OF TABLES	x
1. INTRODUCTION	1
1.1 Cavity Flow	1
1.2 Synthetic Jet Actuator	3
1.3 Principles operation of a synthetic jet	4
2. FUNDAMENTAL EQUATIONS FOR STEADY AND TRANSIENT FLOW IN A CAVITY	5
2.1 Fundamental Equations for Incompressible Unsteady Viscous Flow	5
2.2 The CFD Process	7
2.3 FLUENT/ POINTWISE Description	8
3. COMPUTATIONAL RESULTS FOR STEADY AND UNSTEADY CAVITY FLOWS	11
3.1 Steady Flow in a Cavity	11
3.1.1 Computational Grid and Construction of Geometry	11

3.1.2 Boundary conditions	12
3.1.3 Results	16
3.2 Transient Flow in Cavity	24
3.2.1 Computational Grid and Construction of Geometry:	24
3.2.2 Boundary Conditions:	24
3.2.3 Results	25
3.3 Comparison of Steady Flow and Transient Flow	30
3.4 Synthetic jets in Quiescent flow with air and water	31
3.4.1 Computational grid and construction of geometry:	32
3.4.2 Results	35
3.5 Synthetic Jet in a Cavity with Two Pressure Outlets	37
3.5.1 Computational Grid and Methodology:	37
3.5.3 Results for cavity flow with symmetry	39
3.5.4 Results for Cavity Flow without Symmetry	41
3.6 Comparison of the Cavity Flow Behavior for Symmetry and Non-symmetry	44
3.7 Synthetic jet in velocity inlet and pressure outlet cavity	44

3.7.1 Computational Grid and Geometry	45
3.7.2 Boundary Conditions	46
3.7.3 Results	47
4. CONCLUSION AND FUTURE WORK	51
APPENDIX	54

LIST OF FIGURES

FIGURE 1: GRID GENERATED FOR THE SQUARE CAVITY	13
FIGURE 2: STEADY FLOW IN A CAVITY AT $Re=1$	17
FIGURE 3: STEADY FLOW IN A CAVITY AT $Re=10$	17
FIGURE 4: STEADY FLOW IN A CAVITY AT $Re=100$	18
FIGURE 5: STEADY FLOW IN A CAVITY AT $Re=1000$	18
FIGURE 6: STEADY FLOW IN A CAVITY AT $Re=1100$	19
FIGURE 7: STEADY FLOW IN A CAVITY AT $Re=1200$	19
FIGURE 8: STEADY FLOW IN A CAVITY AT $Re=1300$	20
FIGURE 9: STEADY FLOW IN A CAVITY AT $Re=1400$	20
FIGURE 10: STEADY FLOW IN A CAVITY AT $Re=1500$	21
FIGURE 11: STEADY FLOW IN A CAVITY AT $Re=1600$	21
FIGURE 12: STEADY FLOW IN A CAVITY AT $Re=1700$	22
FIGURE 13: STEADY FLOW IN A CAVITY AT $Re=1800$	22
FIGURE 14: STEADY FLOW IN A CAVITY AT $Re=1900$	23
FIGURE 15: STEADY FLOW IN A CAVITY AT $Re=2000$	23
FIGURE 16: TRANSIENT FLOW IN A CAVITY FOR $\Delta T=10S$	26
FIGURE 17: TRANSIENT FLOW IN A CAVITY FOR $\Delta T=1S$	26
FIGURE 18: TRANSIENT FLOW IN A CAVITY FOR $\Delta T=0.1S$	27
FIGURE 19: TRANSIENT FLOW IN A CAVITY FOR $\Delta T=0.05S$	27
FIGURE 20: TRANSIENT FLOW IN A CAVITY FOR $\Delta T=0.03S$	28
FIGURE 21: TRANSIENT FLOW IN A CAVITY FOR $\Delta T=0.02S$	28
FIGURE 22: TRANSIENT FLOW IN A CAVITY FOR $\Delta T=0.01S$	29
FIGURE 23: COMPARISON OF STEADY (A) AND TRANSIENT FLOW (B) FOR $Re=1700$	31
FIGURE 24: GRID GENERATED FOR THE SYNTHETIC JET IN AIR	34

FIGURE 25: PRESSURE AT PEAK SUCTION OF SYNTHETIC JET	36
FIGURE 26: PRESSURE AT PEAK BLOWING OF SYNTHETIC JET	36
FIGURE 27: GRID GENERATED FOR THE SYNTHETIC JET WITH TWO PRESSURE OUTLETS	38
FIGURE 28: SYMMETRIC CAVITY FLOW AT TIME= 5S	39
FIGURE 29: SYMMETRIC CAVITY FLOW AT TIME= 10S	40
FIGURE 30: SYMMETRIC CAVITY FLOW AT TIME= 15S	40
FIGURE 31: SYMMETRIC CAVITY FLOW WITH AT TIME =20S	41
FIGURE 32: CAVITY FLOW WITHOUT SYMMETRY AT TIME =5S	42
FIGURE 33: CAVITY FLOW WITHOUT SYMMETRY AT TIME= 10S	42
FIGURE 34: CAVITY FLOW WITHOUT SYMMETRY AT TIME= 15S	43
FIGURE 35: CAVITY FLOW WITHOUT SYMMETRY AT TIME= 20S	43
FIGURE 36: COMPARISON OF THE CAVITY FLOW BEHAVIOR FOR SYMMETRY AND NON- SYMMETRY	44
FIGURE 37: GRID GENERATED FOR THE SYNTHETIC JET LOCATED ON THE TOP RIGHT CORNER	45
FIGURE 38: GRID GENERATED FOR THE SYNTHETIC JET LOCATED ON THE BOTTOM RIGHT CORNER	46
FIGURE 39: VELOCITY AMPLITUDE $V_j= 0.002135$ M/S	47
FIGURE 40: VELOCITY AMPLITUDE $V_j= 0.001708$ M/S	48
FIGURE 41: VELOCITY AMPLITUDE $V_j= 0.0014$ M/S	48
FIGURE 42: VELOCITY AMPLITUDE $V_j=0.004270$ M/S	49
FIGURE 43: VELOCITY AMPLITUDE $V_j= 0.0085408$ M/S	49
FIGURE 44: VELOCITY AMPLITUDE $V_j=0.00085408$ M/S	50

LIST OF TABLES

TABLE 1: BOUNDARY CONDITION OF STEADY FLOW IN CAVITY	12
TABLE 2: VARIATION OF REYNOLDS NUMBER WITH VELOCITY	15
TABLE 3: BOUNDARY CONDITIONS OF TRANSIENT FLOW IN CAVITY	24
TABLE 4: REYNOLDS NUMBER WITH Δt	25
TABLE 5: BOUNDARY CONDITION FOR SYNTHETIC JET IN AIR AND WATER	32
TABLE 6: BOUNDARY CONDITION OF SYNTHETIC JET IN CAVITY	37
TABLE 7: JET IN CAVITY WITH DIFFERENT FLOW TIME AND OF REYNOLDS 10^4	38
TABLE 8: SUMMARY OF THE BOUNDARY CONDITIONS USED FOR SYNTHETIC JET IN SQUARE CAVITY	46

1. INTRODUCTION

1.1 Cavity Flow

The Presence of cavity in a surface bounding a fluid flow can cause large fluctuations of pressure, velocity and density in the flow in its vicinity. Study on the cavity flows has been an area of active research and renewed significance in the past few years. In this case, the control volume is limited. Therefore, a small number of grid nodes are required and simple boundary conditions are set. In the earliest renditions of this problem, the Navier–Stokes equations are transformed into vorticity and stream function variables, which are more convenient for computational methods. When computers appeared, the indicated problem remained, as before, the focus of attention of specialists developing computational methods. A detailed analysis of methods concerning the problem considered that appeared in the period from the 1960s to the late 1980s is given in a set of monographs. One of the first works in the area of numerical investigation of a viscous-fluid flow in a square cavity began thirty years ago on a BESM-4 computer containing 21×21 grid nodes in one memory cube. At that time, in the mid-1970s, high-accuracy schemes (Arakava, 1970) of the second and fourth order of approximation and non-uniform grids were used for the first time for solving Navier–Stokes equations. Progress in computational methods and, especially, widespread use of personal computers in the 1980's and subsequent years have made it possible, first of all, to develop universal codes of applied programs, such as PHOENIX, FLOW3D, and FIDAP, and then more modern products / commercial CFD

codes such as FLUENT, StarCD, and CFX. When computers with large memory and high speed CPU appeared, instead of the Navier– Stokes equations in transformed variables, they were predominantly written in terms of the actual physical variables, velocity and pressure components. This made it possible to increase the number of computational cells (by an order of magnitude and more) and to increase the resolution in the near-wall region for this problem [Isaev, 2005, 2006].

Cavities are divided into two types, open and closed [Debiasi, 2011]. Open flow regimes exhibit distinct peak in measured sound pressure spectra, whilst closed cavity signals are more broadband. Open cavities refer to flow over cavities where the boundary layer separates at upper stream corner and reattaches near the downstream corner. Cavities are closed when separated layer reattaches at the bottom again separates a head of downstream wall. Open cavities are divided into shallow and deep [Debiasi, 2011]. In high performance military aircraft the acoustic environment that can exist in open cavity can be a severe design constraint [Borland, 1977].

Flow over cavities is of interest, because presence of cavities changes drag and heat transfer and may cause intense periodic oscillations. In particular, cavity flow has specific relevance to the drag experienced on many aerodynamic bodies. This is exemplified through the presence of numerous cavities like geometries on standard aircraft, including cargo bays and landing gear enclosures. These flow disruptions resulting in adverse pressure gradients have a significant effect on the overall drag of a body [Fernando, 2014]. Some of the controlling methods used to stabilize flow over a square cavity

[Barbagallo, 2008]. Some application on cavities over SCRAMJET [Baurle, 2000] and cavities exposed to grazing flows can be found in many industrial applications, especially in ground ,air and maritime transportation. The study of shear layer developing from the upper stream edge of the cavity, the consequent vortex shedding and the generation of recirculation zones. This phenomenon play a relevant role into the generation of noise, drag, Pressure fluctuation and structural vibration [Verdugo, 2012].

1.2 Synthetic Jet Actuator

Active flow control using synthetic jets has received people's attention in recent years. It deals with suction and blowing into the boundary layer. The addition of energy into the flow allows the "new" boundary layer to overcome the adverse pressure gradient and therefore delay separation. The drag coefficient can be significantly decreased by shifting the transition point in the boundary layer in the downstream direction by using suction. On the other hand, additional energy is supplied to the fluid particles in the boundary layer by blowing which enhances the mixing of blowing fluid and oncoming flow within the boundary layer. The use of oscillatory blowing and suction has been found to be more effective than just steady blowing or steady suction alone. The first description of a device similar to "synthetic jet actuator" was given by Ingard, 1953[Mohamed,2000]; however, in the recent years there have been significant advances in the development of "synthetic jet" or "zero-net-mass-flux" actuators which are widely used for a variety of flow control

applications. These actuators require low energy for operation although they are small in size, low weight and low cost. They can be easily integrated into the surface of the object as needed e.g. into an airplane wing.

1.3 Principles operation of a synthetic jet

A typical actuator consists of a cavity open at the top by a small slit through which fluid is free to flow. The flow inside the cavity is driven by a moving surface, either an oscillating piston or a vibrating diaphragm. The oscillation of the diaphragm produces a fluctuation of the pressure field in the cavity and at the exit slit, causing it to periodically act as a source and a sink. This

Behavior results in a jet originating from the slit. A non-zero momentum is imparted to the external flow even though there is no net mass injected during a cycle. The slit is the only communication between the cavity of the actuator and the external flow. Ambient fluid from the external flow enters the cavity and exits the cavity in a periodic manner. Upward motion of the diaphragm generates flow which separates at the sharp edges of the slit and rolls into a pair of vortices generated at the two edges of the slit. These vortices then move away from the slit at their own induced velocity [David, 1987].

In past there is no more research on synthetic jet in cavity to control vortex in this research it is studied the influence of synthetic on vortex in cavity based on previous research on synthetic jet a series of attempts has been done to see the influence of synthetic jet.

2. FUNDAMENTAL EQUATIONS FOR STEADY AND TRANSIENT FLOW IN A CAVITY

The overall goal of this research is to study the transient flow in a square cavity. This was also followed by some minor study on synthetic jet in square cavity and its influence on vortex inside the cavity. To achieve the primary goal, a series of cases are designed and meshed in POINTWISE and simulation are done in Computational Fluid Dynamics (CFD) and results have been discussed in all cases, A series of cases studied are

1. Steady square cavity flow
2. Transient square cavity flow
3. Synthetic jets in quiescent flow (Air and Water)
4. Synthetic jet in a cavity
5. Synthetic jet in square cavity flow

2.1 Fundamental Equations for Incompressible Unsteady Viscous Flow

Computational Fluid Dynamics (CFD) method comprises of solution of Navier Stokes equations at required points to get the properties of the fluid flow at those points. Simple fluid flow problems were solved analytically, but with the increase in fluid flow complexity, mathematical difficulties increased significantly. With 3D interactive capability and powerful graphics, use of CFD has gone beyond research and into industry as a design tool.

The governing equations for computational fluid dynamics are based on conservation of mass, momentum and energy. Fluent uses a Finite Volume Method (FVM) to solve the governing equations. The FVM involves discretization and integration of the governing equation over the control volume [Ghia, 1982].

The basic equations for unsteady-state incompressible laminar flow are conservation of mass and momentum. When heat transfer or compressibility is involved the energy equation is also required. The governing equations are:

Continuity equation

$$\frac{\partial u}{\partial x} + \frac{\partial v}{\partial y} = 0 \quad (1)$$

Conservation of momentum:

X-Momentum

$$\rho \left(\frac{\partial u}{\partial t} + u \frac{\partial u}{\partial x} + v \frac{\partial u}{\partial y} \right) = - \frac{\partial p}{\partial x} + \mu \left(\frac{\partial^2 u}{\partial x^2} + \frac{\partial^2 u}{\partial y^2} \right) \quad (2)$$

Y-Momentum

$$\rho \left(\frac{\partial v}{\partial t} + u \frac{\partial v}{\partial x} + v \frac{\partial v}{\partial y} \right) = - \frac{\partial p}{\partial y} + \mu \left(\frac{\partial^2 v}{\partial x^2} + \frac{\partial^2 v}{\partial y^2} \right) \quad (3)$$

At the walls no slip condition, boundary conditions and initial conditions for all the cases are mentioned below.

2.2 The CFD Process

A brief outline of the process for performing a CFD analysis is given in this section. Several steps are required for modeling fluid flow using CFD. Essentially, there are three main stages in every simulation process: preprocessing, flow simulation and post-processing. Preprocessing is the first step in building and preparing a CFD model for the flow simulation step. This included the problem specification and construction of the computer model via computer-aided design software. Once the computer model is constructed, a suitable grid or mesh is created in the computational domain. Then the flow conditions including the material properties of the fluid such as density, viscosity, thermal conductivity, etc. are specified.

The computational domain should be chosen in such a way that an acceptably accurate answer is obtained without excessive computations being required. The nature of the flow-field and the geometry generally provides a guide for a suitable mesh construction as to its structure (structured, unstructured, zonal or hybrid) and topology (c-, o-, h- or hybrid). There is also an option to adapt the mesh according to the solution. It can automatically cluster in regions of higher flow gradients by sensing the solution as it evolves. A good mesh should display qualities such as orthogonally, lack of skewness and gradual spacing to obtain accurate solutions.

All the above mentioned steps constitute the preprocessing prior to the second step of flow simulation, in which the boundary conditions and initial conditions of the problem must be specified. For the second step, the mesh coordinates the boundary conditions in the computational domain and the material properties of the fluids are imported into a flow solver such as FLUENT. The flow solver then executes the solution process for solving the governing equations of the fluid flow. The governing equations are solved employing a suitable numerical algorithm which is coded in the flow solver. As the solution process proceeds, the solution is monitored for convergence implying that there is little change in the solution from one solution step to the next. Once the solution within a specified error tolerance is obtained, the post-processing step begins.

This step involves the display of converged flow variables in graphical and animated forms. Computed flow properties are then compared with the experimental data (if available) or with the computations of other investigators to validate the solutions. The simulation is complete at this point although, a sensitivity analysis of the results is recommended to understand the possible differences in the accuracy of the results with variations in the mesh size and the other parameters used in the algorithms.

2.3 FLUENT/ POINTWISE Description

FLUENT is the worlds' largest provider of commercial CFD software and services. FLUENT software contains the broad physical modeling capabilities needed to model flow, turbulence, heat transfer and reactions for industrial applications ranging from air

flow over an aircraft wing to combustion in a furnace, from bubble columns to oil platforms, from blood flow to semiconductor manufacturing, and from clean room design to wastewater treatment plants. Special models that give the software the ability to model in-cylinder combustion, aero acoustics, turbo machinery and multiphase systems have served to broaden its reach. FLUENT can be used to solve complex flows ranging from incompressible (subsonic) to highly compressible (supersonic or hypersonic) including the transonic regime. FLUENT provides mesh flexibility, including two-dimensional triangular/quadrilateral meshes and three-dimensional tetrahedral, hexahedral or hybrid meshes. The grid can also be refined or coarsened based on the flow solution using the grid adaptation capability. Furthermore, it provides multiple solver options, which can be modified to improve both the rate of convergence of the simulation and the accuracy of the computed result. The software code is based on the finite volume method and has a wide range of physical models which allow the user to accurately predict laminar and turbulent flows, chemical reactions, heat transfer, multiphase flows and other related phenomena.

A fluid flow domain geometry can be created in CAD software like CATIA or Pro-Engineer and imported in mesh generating software like POINTWISE, GRIDGEN, GAMBIT etc. For this research since the geometry is not complicated it is created and meshed in POINTWISE. POINTWISE is flexible, robust and reliable software for mesh generation. POINTWISE provides high mesh quality to obtain converged and accurate CFD solutions especially for viscous flows over complex geometry.

Mesh generation, also known as grid is the process of forming nodes across the geometry. Nodes are the points at which the Navier-Stokes equations will be solved for the fluid properties. When these nodes are connected, a mesh is formed and the domain or the control volume is called discretized. There are several aspects to be considered for mesh generation. First is the type of the mesh. There are two main type of mesh: Structured and Unstructured. A structured mesh has all the nodes arranged such that the cells formed by joining adjacent nodes are rectangular in shape. This helps in easy reference of each cell making it numerically simple to deal with. An Unstructured mesh has nodes distributed randomly; hence the mesh cells can be tetrahedral, octahedral and pyramid in shape for 3D mesh and triangular in shape for 2D mesh. This random arrangement of nodes require a mapping file to keep the track of the nodes, increasing the file size of unstructured mesh compared to structured mesh. Unstructured mesh is useful for meshing complex and curved geometries. Since we are dealing with 2D flat structured mesh is used. Once the model is meshed, the boundary conditions are specified in POINTWISE.

3. COMPUTATIONAL RESULTS FOR STEADY AND UNSTEADY CAVITY FLOWS

3.1 Steady Flow in a Cavity

The research mainly focusses on the laminar fluid flow over the cavities with the influence of Reynolds number. The fluid dynamic interactions with the growth of shear layer and the formation of vortices in the cavities are observed. The Reynolds Number is varied and the influence on the vortex formation is investigated. A small square cavity is considered with an inlet and outlet, constituting same dimensions. The water is injected at a certain velocity and the vortex formation is observed. A series of velocities are induced with the variation of Reynolds Numbers, and a mesh generation and method implanted in fluent setup is studied.

3.1.1 Computational Grid and Construction of Geometry

A square of dimension 20cm X 20cm is constructed using POINTWISE. POINTWISE is software which generates mesh for the computational fluid dynamics. As mentioned earlier, the inlet and outlet constituting 1cm each are generated top ends of the cavity. Each connector is divided into 200 points and structured grid is generated in the domain as shown in the figure below. A structured grid is preferred as mesh quality is the key for the CFD solutions. The grid designates the cells or elements on which the flow is solved. It is a discrete representation of the geometry of the problem. Has cells grouped into boundary zones where boundary conditions are applied. The geometry describes the shape of the

problem to be analyzed. Geometries can be created top-down or bottom up. Top-down refers to an approach where the computational domain is created by performing logical operations on primitive shapes such as cylinders, bricks, and spheres. Bottom-up refers to an approach where one first creates vertices (points), connects those to form edges (lines), connects the edges to create faces, and combines the faces to create volumes .Once the structured grid is produced, the boundary conditions are assigned.

3.1.2 Boundary conditions

Table 1: Boundary condition of steady flow in cavity

Boundary conditions	Number of connectors
Velocity inlet	1
Pressure outlet	1
Wall	4

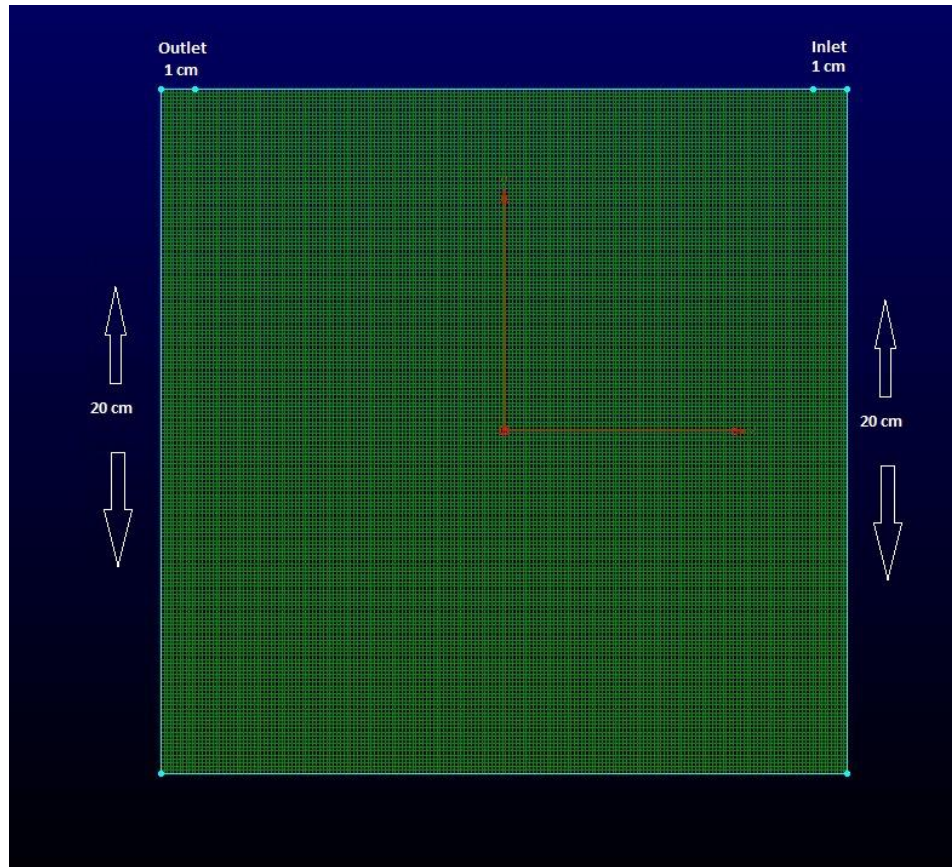


Figure 1: Grid generated for the square cavity

- Velocity inlet boundary conditions are used to define the velocity and scalar properties of the flow at inlet boundaries.
- Pressure outlet boundary conditions are used to define the static pressure at flow outlets. The use of a pressure outlet boundary condition instead of an outflow condition often results in a better rate of convergence when backflow occurs during iteration.
- Wall boundary conditions are used to bound fluid and solid regions. In viscous flows, the no-slip boundary condition is enforced at walls by default. Ansys Fluent

Solver is selected for the cavity domain to be solved. The file is then exported into fluent.

Once the mesh is generated and all conditions are given it is saved as a .CAE file then open the .CAE file and select 2D and double precision and display mesh once it is done fluent allows us to change the mesh scale option where we can change mesh scale according to our need the mesh check as to be done. And in initial condition pressure based solver is selected followed by steady flow and viscous laminar for simulation, water is selected in material Reference values are computed from the velocity inlet Standard pressure and first order upwind momentum spatial discretization is chosen as solution methods Relaxation factors are set at default values, Then the solution is initialized Then solution is calculated. Once the solution is converged post results were analyzed in TECPLOT. The pressure, vorticity and velocity contour plots were obtained and velocity stream lines plotted.

The same methodology is followed for the further analysis and the Reynolds Number is varied from 1 to 2000 at a certain interval. The velocities with the variation of Reynolds Number are shown below:

Table 2: Variation of Reynolds number with velocity

Reynolds numbers	Velocity in m/s
1	5.024×10^{-6}
10	5.024×10^{-5}
100	5.024×10^{-4}
1000	5.024×10^{-3}
1100	0.0055264
1200	0.0060288
1300	0.0065312
1400	0.007033
1500	0.007536
1600	0.008038
1700	0.0085408
1800	0.009043
1900	0.009545
2000	0.010048

The FLUENT Analysis is accomplished at each respective Reynolds Number and the vortex formation is observed. The following images shows the velocity contours with the streamlines plotted for examining the formation of vortices.

3.1.3 Results

Flow in a cavity is an interesting study it is seen in research the behavior of vortex changes with varying Reynolds number. The variation of Reynolds with their velocity are shown in Table 2 the following images shows the velocity contours with stream lines and explained in detail.

The formation of vortex and the contours are similar for the Reynolds Numbers 1, 10 and 100. A small vortex is formed in the top right corner of the cavity along with the strong vortex which exists in the bottom left corner. With the increase in the Reynolds number the size and the strength of the vortex in the top right starts increasing from Reynolds Number 1000. Simultaneously the size and strength of the bottom left corner vortex decreases. At Reynolds Number 1700, the bottom left corner vortex is eliminated completely. A small vortex starts growing in the right end and starts building its strength from Reynolds Number 1500. The Reynolds Number is further increased after 1700, both the vortices starts increasing their size and strength. The center of the top right vortex kept shifting towards the center of the square cavity with increase in the Reynolds.

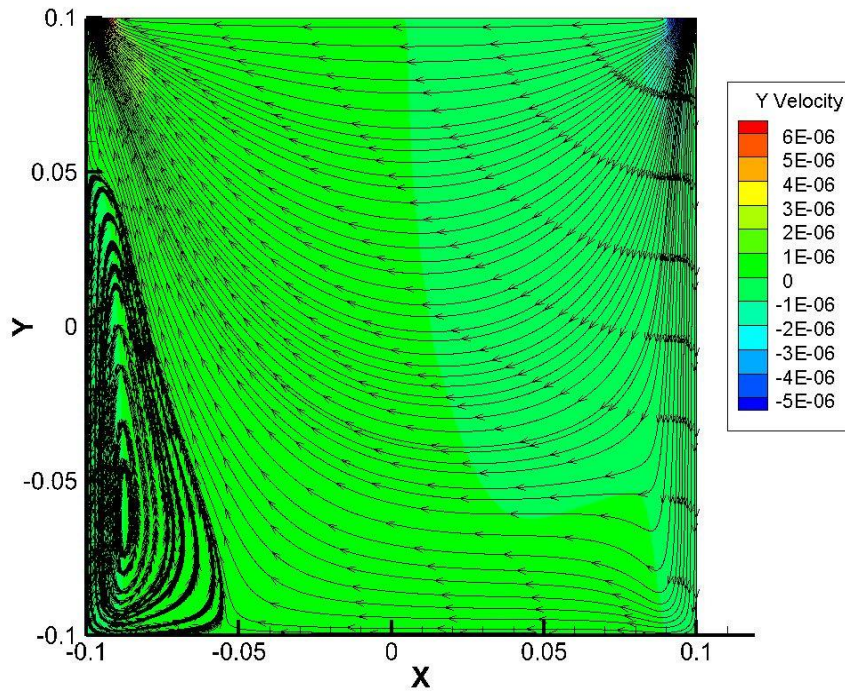


Figure 2: Steady flow in a cavity at $Re=1$

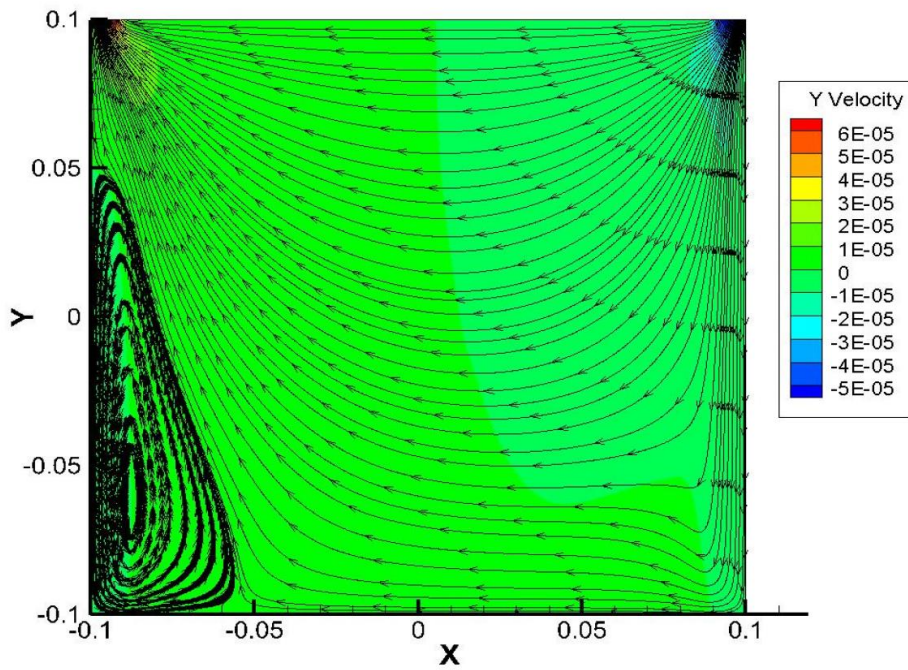


Figure 3: Steady flow in a cavity at $Re=10$

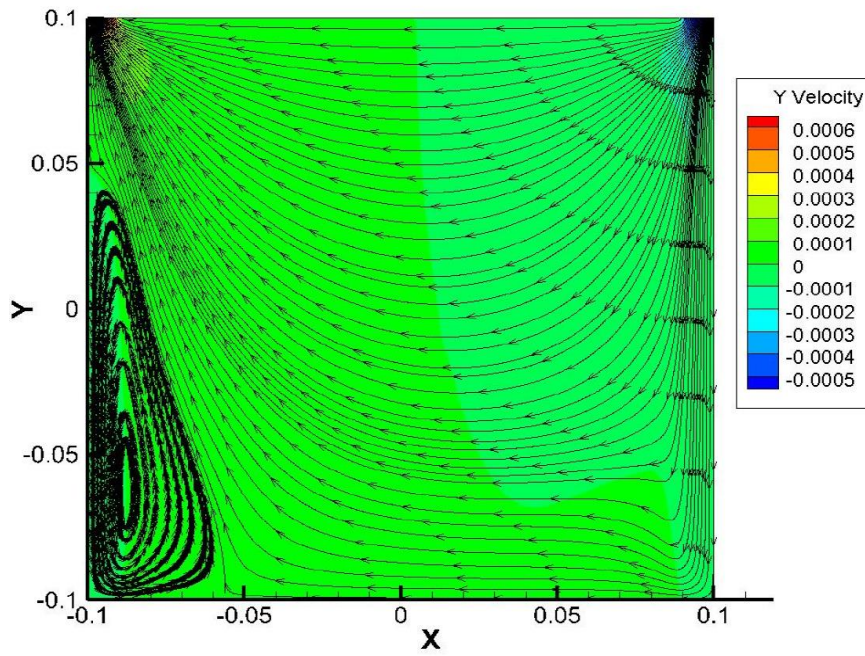


Figure 4: Steady flow in a cavity at $Re = 100$

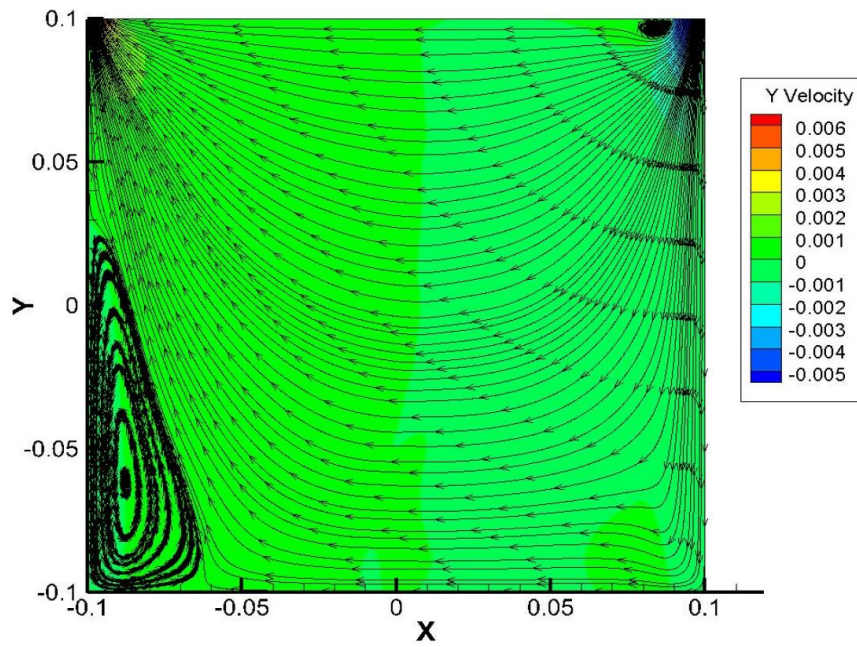


Figure 5: Steady flow in a cavity at $Re = 1000$

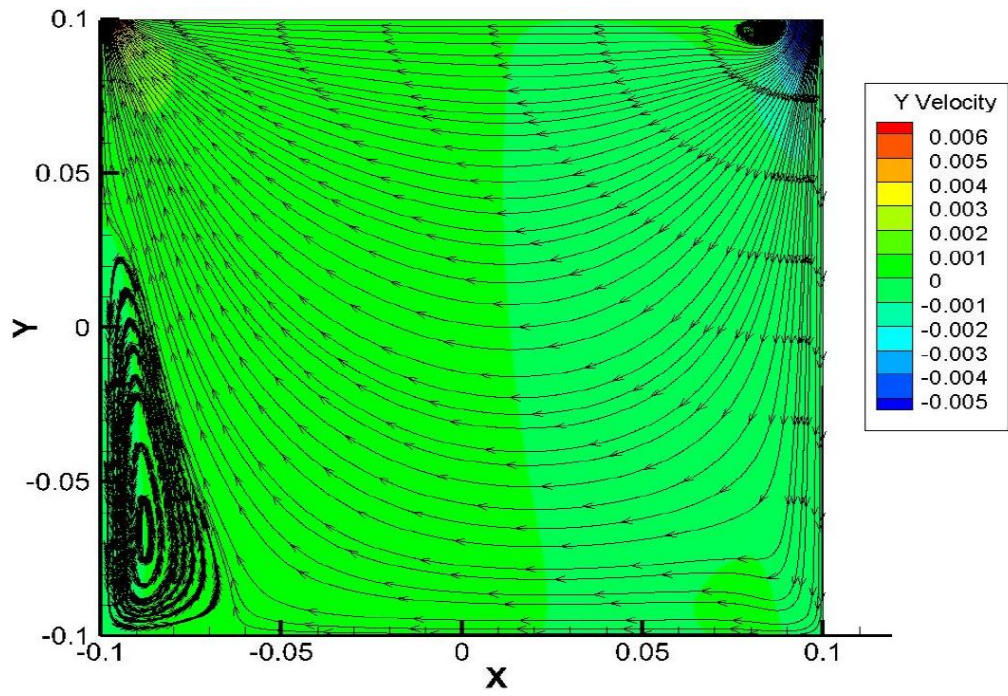


Figure 6: Steady flow in a cavity at $Re = 1100$

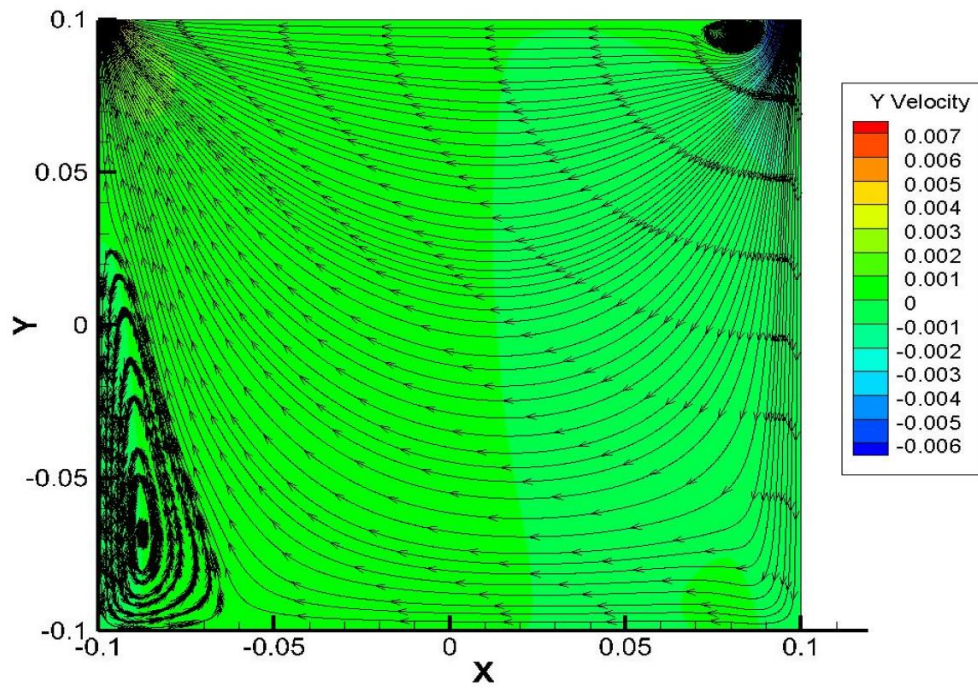


Figure 7: Steady flow in a cavity at $Re = 1200$

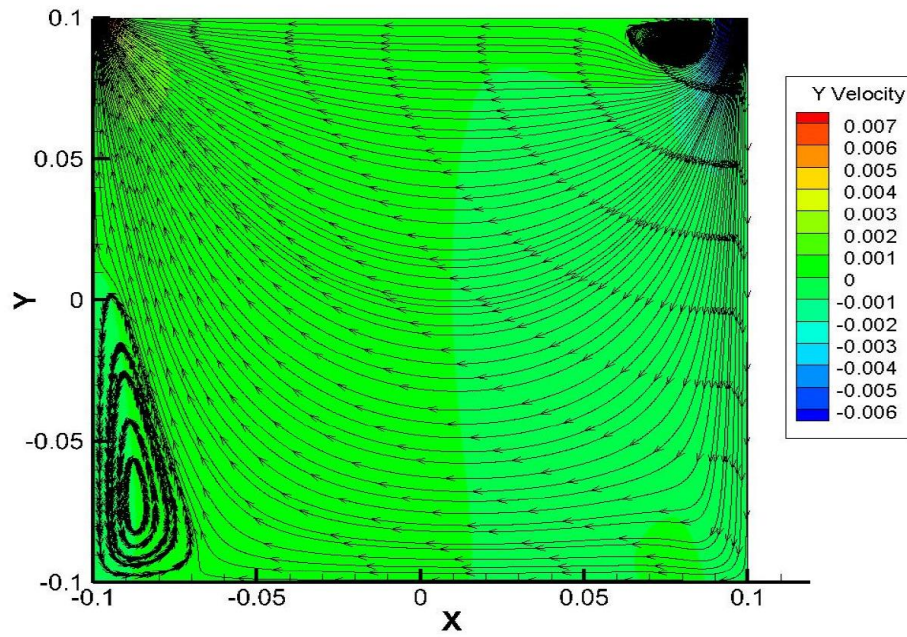


Figure 8: Steady flow in a cavity at $Re = 1300$

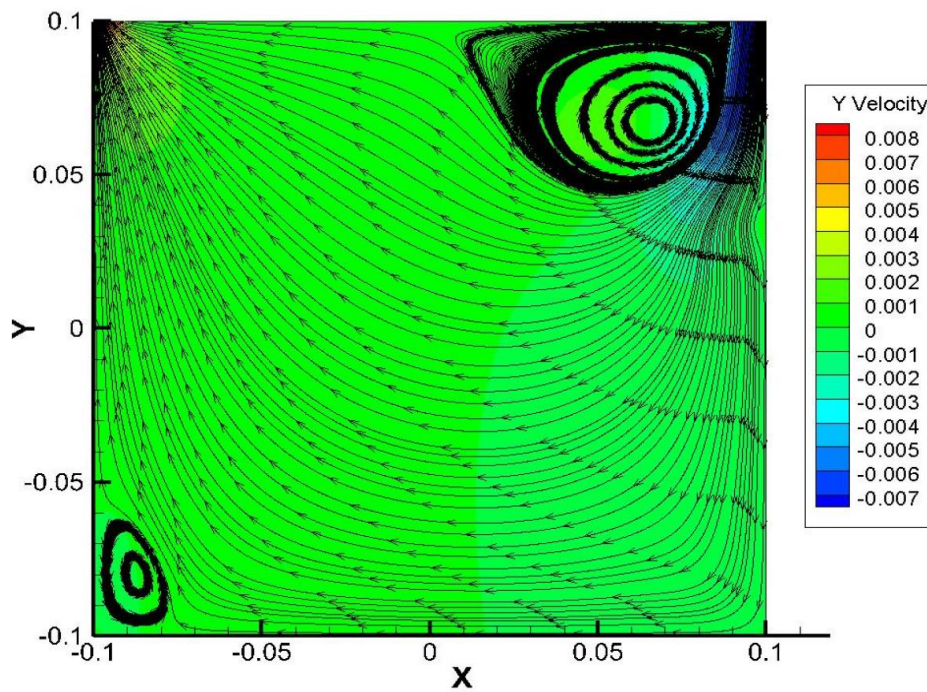


Figure 9: Steady flow in a cavity at $Re = 1400$

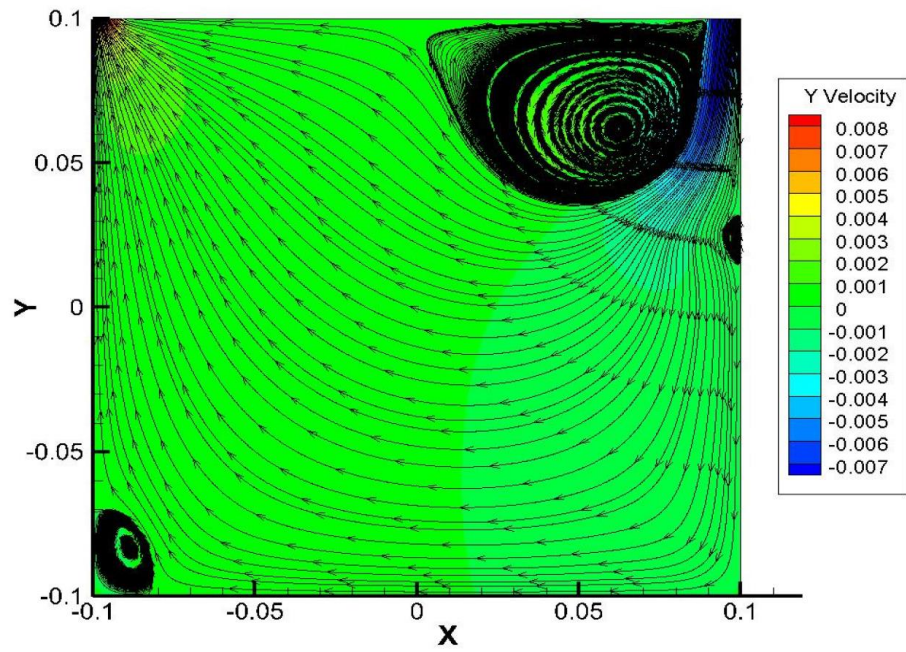


Figure 10: Steady flow in a cavity at $Re = 1500$

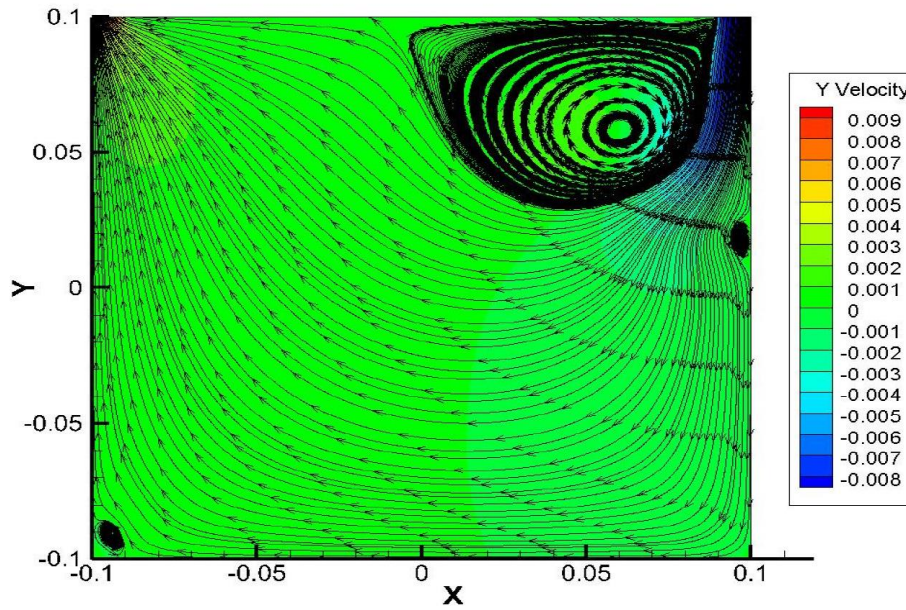


Figure 11: Steady flow in a cavity at $Re = 1600$

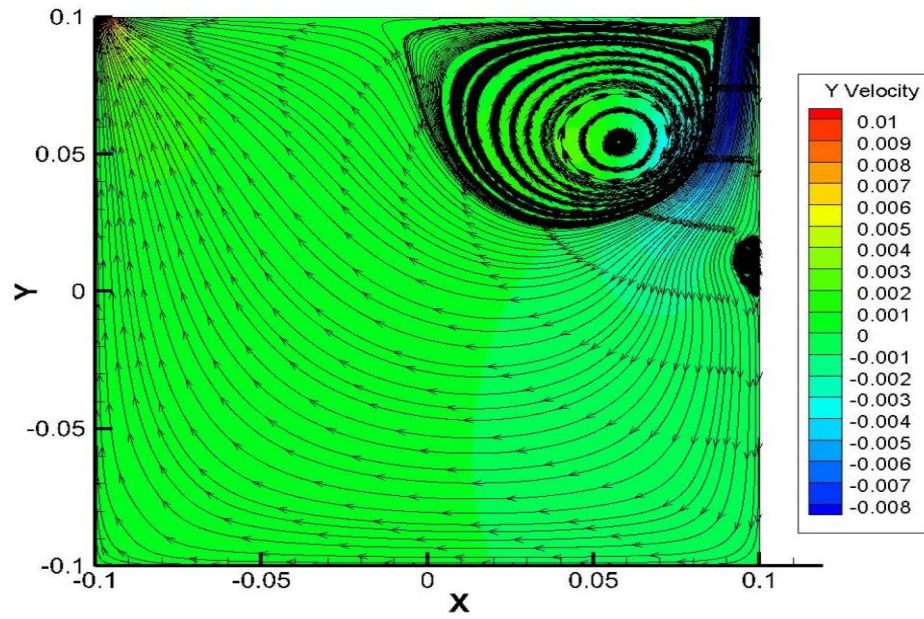


Figure 12: Steady flow in a cavity at $Re = 1700$

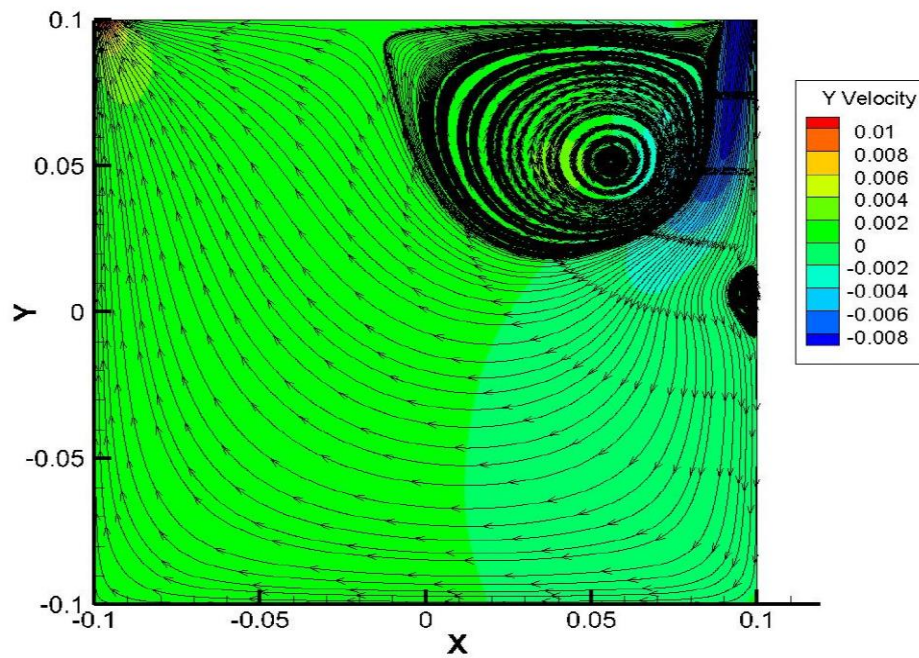


Figure 13: Steady flow in a cavity at $Re = 1800$

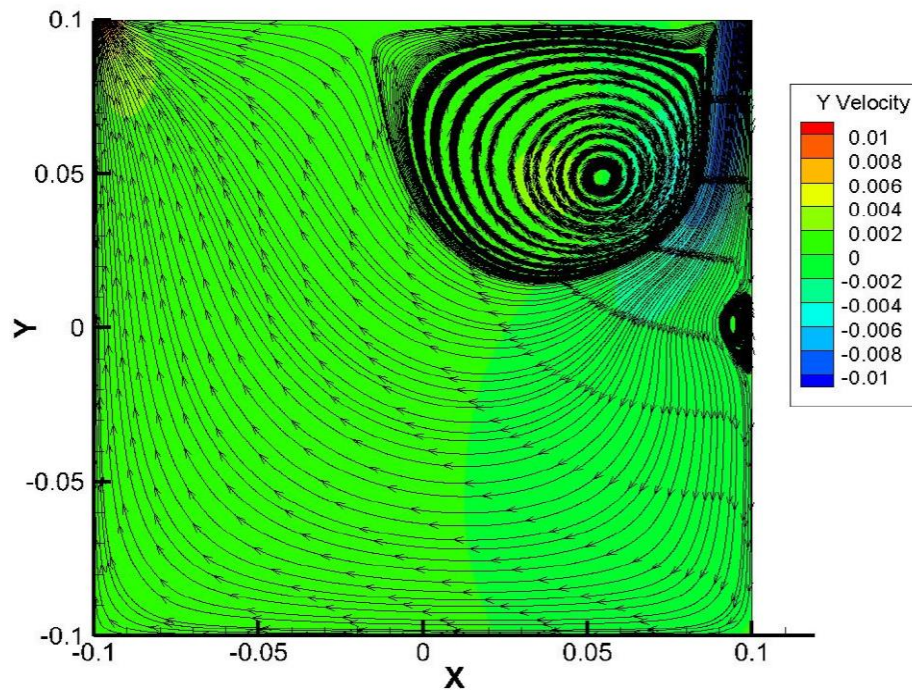


Figure 14: Steady flow in a cavity at $Re = 1900$

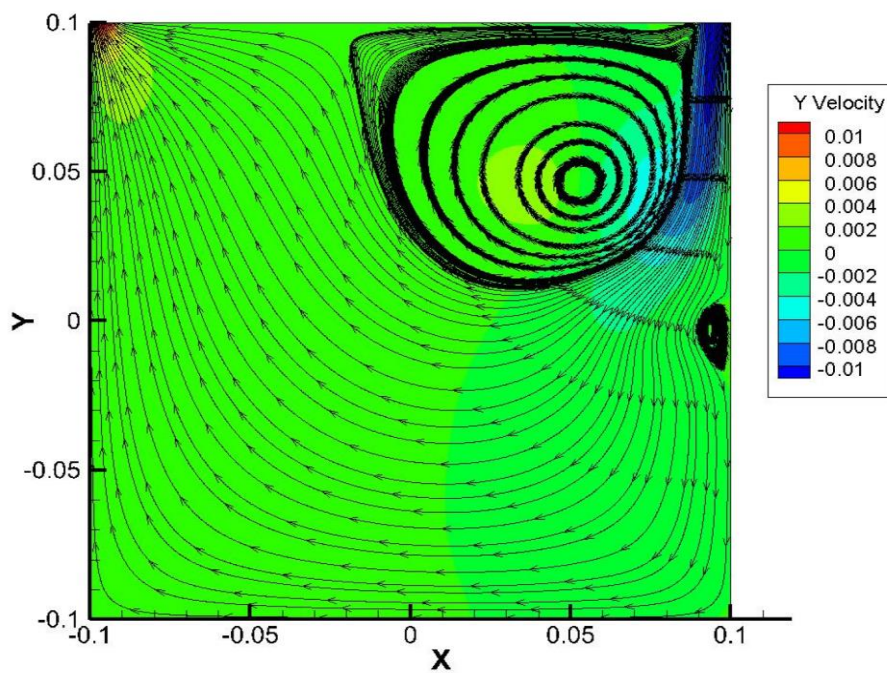


Figure 15: Steady flow in a cavity at $Re = 2000$

3.2 Transient Flow in Cavity

This section of the research focuses on a transient flow inside the cavity, where a Reynolds number of 1700 is maintained for the simulation. The result is compared with the simulation results for the steady flow inside the cavity at the same Reynolds number. The comparison focuses on the flow time as the results are varied by the time step size, Δt . A generation of mesh and geometry remains same as steady flow whereas in fluent Δt is varied and transient is selected for simulation.

3.2.1 Computational Grid and Construction of Geometry:

A geometry and grid is unchanged a same geometry of steady flow is used for this unsteady case, Boundary condition remained same but time delta t has be varied for the same Reynolds.

3.2.2 Boundary Conditions:

Table 3: Boundary conditions of transient flow in cavity

Boundary conditions	Number of connectors
Velocity inlet	1
Pressure outlet	1
Wall	4

In fluent the method is followed same as steady case just changing the steady to transient flow and Δt has been varied for same Reynolds number and results has been plotted.

3.2.3 Results

As it is understood from the previous section, the same geometry has been taken for this case and Reynolds of 1700 is selected and case is studied in detail. An interesting behavior of vortex inside the cavity is seen.

A Reynolds of 1700 is used for simulation in which it varies with Δt and velocity contours are plotted with stream lines for different Δt . Table 4, below shows the Reynolds number and flow time.

Table 4: Reynolds number with Δt

Reynolds number	Δt (s)
1700	10 s
1700	1
1700	0.1
1700	0.05
1700	0.03
1700	0.02
1700	0.01

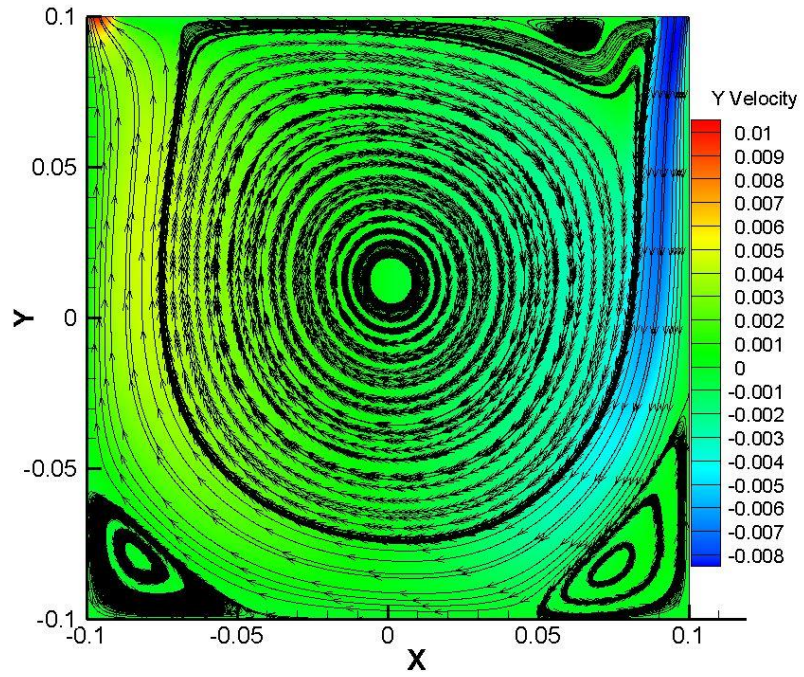


Figure 16: Transient flow in a cavity for $\Delta t= 10s$

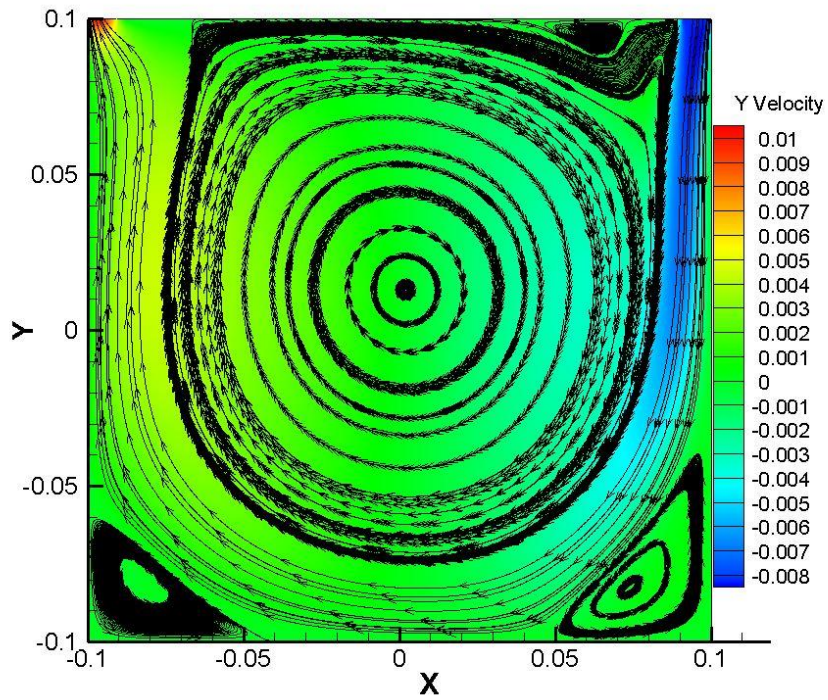


Figure 17: Transient flow in a cavity for $\Delta t= 1s$

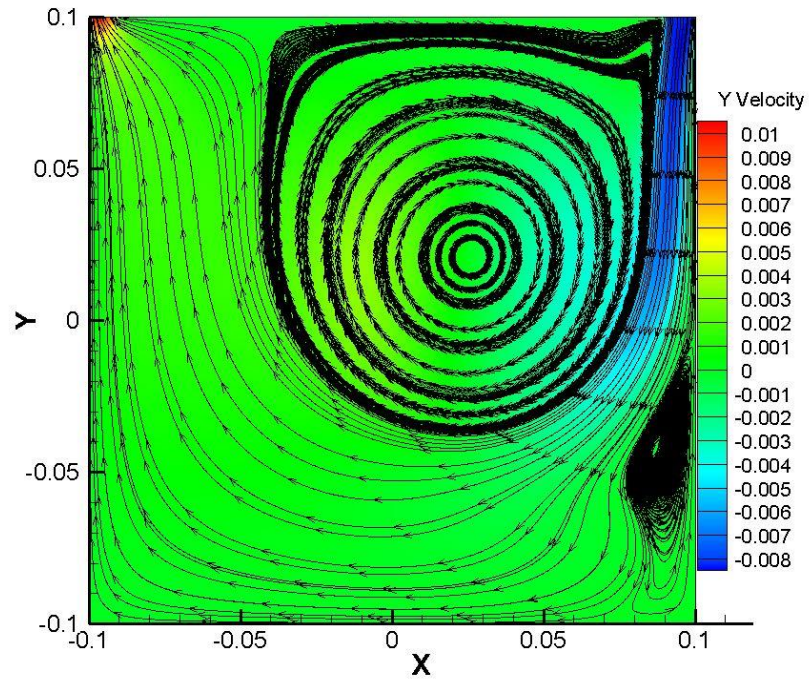


Figure 18: Transient flow in a cavity for $\Delta t = 0.1s$

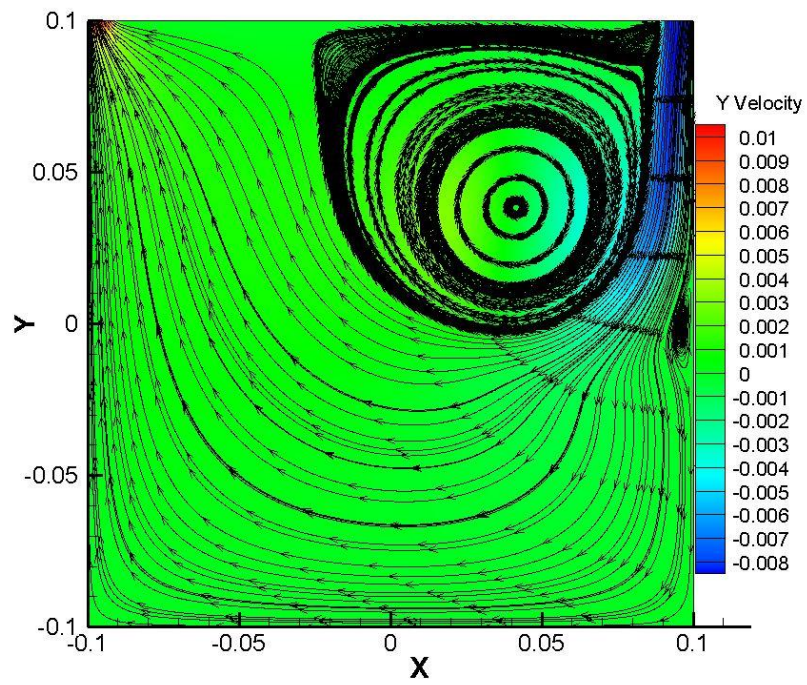


Figure 19: Transient flow in a cavity for $\Delta t = 0.05s$

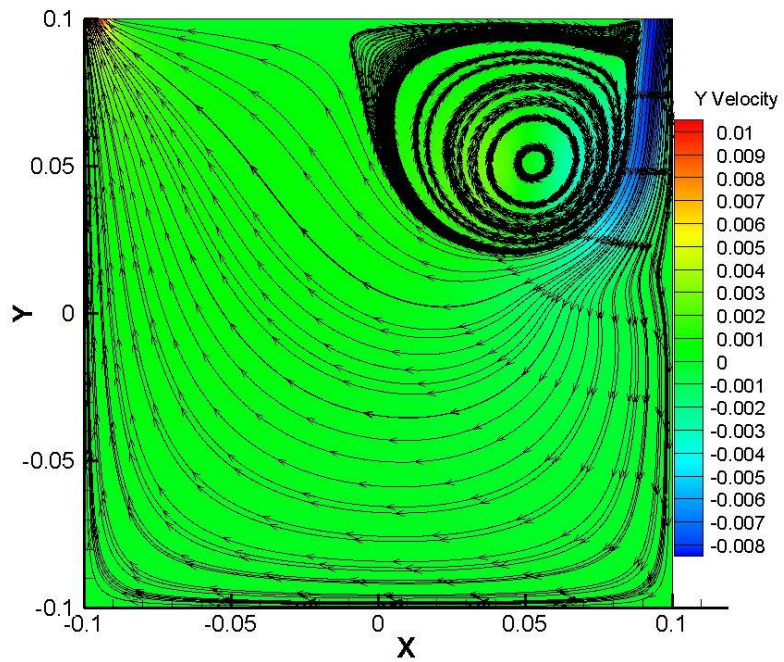


Figure 20: Transient flow in a cavity for $\Delta t = 0.03s$

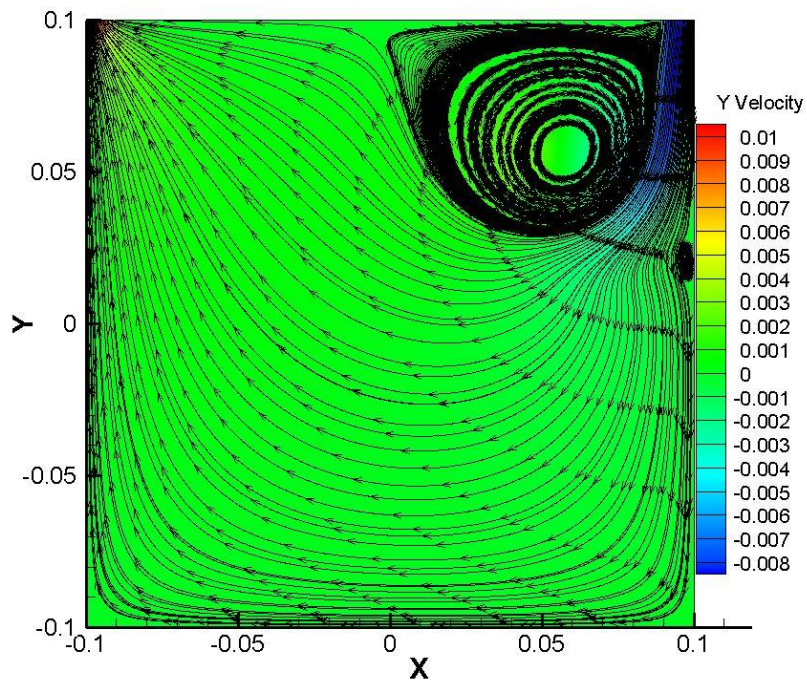


Figure 21: Transient flow in a cavity for $\Delta t = 0.02s$

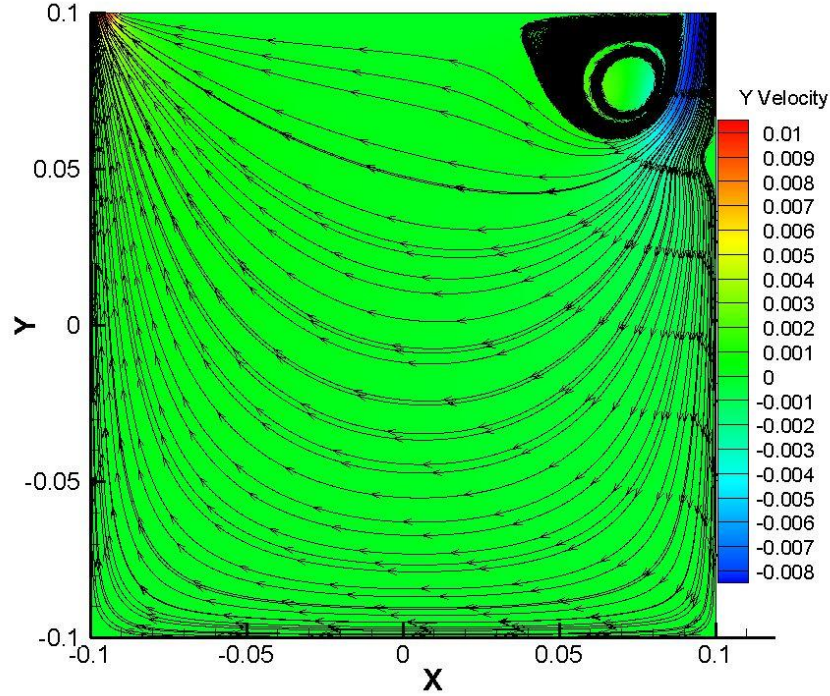
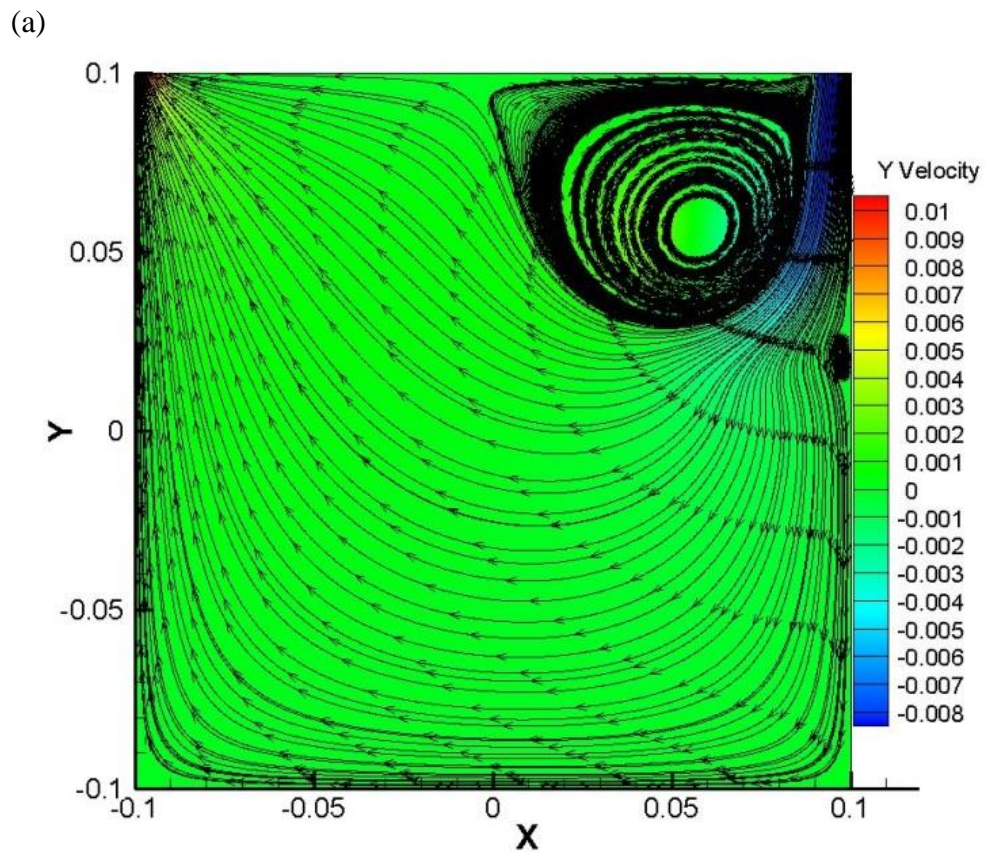


Figure 22: Transient flow in a cavity for $\Delta t = 0.01s$

The simulation is carried out at a Reynolds number of 1700 by varying the time step Δt . It is observed that for $\Delta t = 10s$ a large unstable strong vortex is formed in the center with two small vortices at bottom to left and right. For $\Delta t = 1s$, the large vortex at center remained same but the left and right bottom vortices start to deform further for values of Δt smaller than 0.1s. It is observed that the large center vortex start to decrease in size and the two small vortices disappear. However, the large vortex still remains unstable as Δt is further reduced to 0.05s, 0.03s, 0.02s, and 0.01s. It is also observed that the solution does not converge at 0.05s, 0.03s, and 0.01s, but the solution is converged to steady at 0.02s. It is seen that there is a significant influence of time step on the stability of vortices.

3.3 Comparison of Steady Flow and Transient Flow

A steady flow is observed for Reynolds 1700 as shown in Figure 23 (a). Here the solution is converged and a small vortex at the right is formed and it is a similar feature is that is observed for the transient flow with Reynolds 1700 and with a time step size $\Delta t=0.02s$ which is shown in Figure 23 (b).



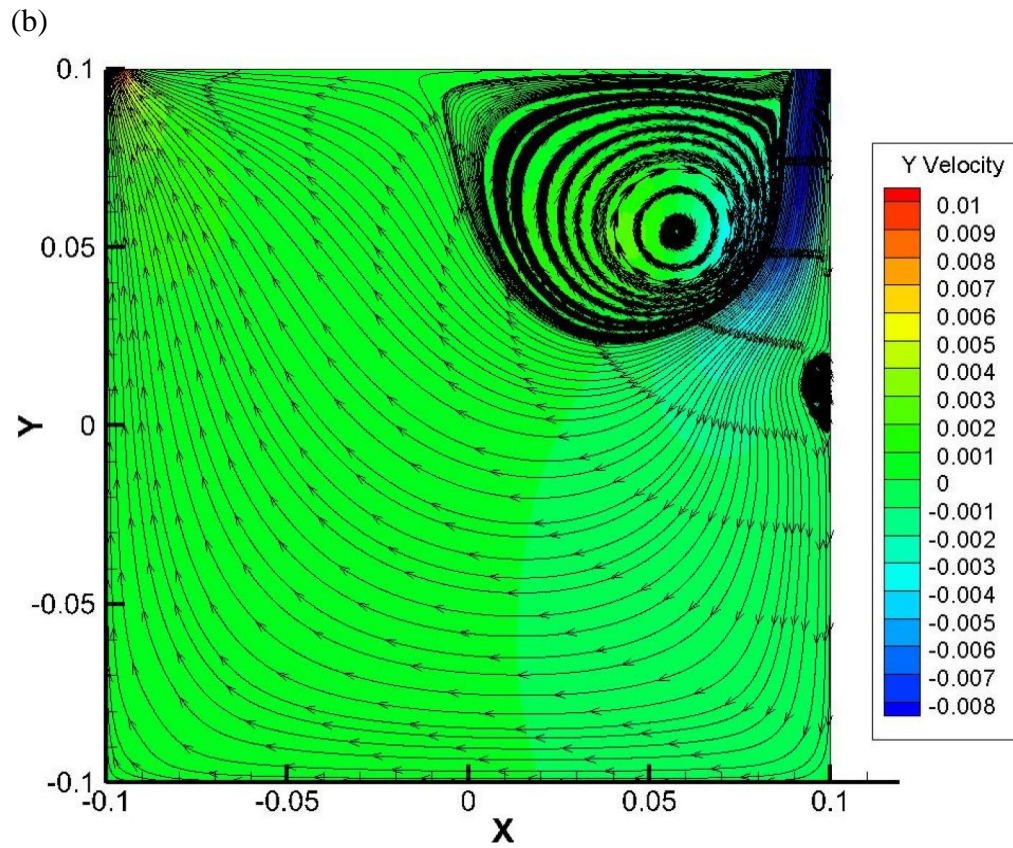


Figure 23: Comparison of steady (a) and transient flow (b) for $Re\ 1700$

3.4 Synthetic jets in Quiescent flow with air and water

The simulation plays a very important role in saving time and cost this chapter gives details about the method of grid generation and geometry followed by boundary condition and fluent simulation set up.

3.4.1 Computational grid and construction of geometry:

POINTWISE is flexible, robust and reliable software for mesh generation. POINTWISE provides high mesh quality to obtain converged and accurate CFD solutions especially for viscous flows over complex geometry. A $0.2\text{m}\times 0.6\text{m}$ cavity is created with a depth of 0.05m and a length of 0.05m . This small cavity functions as a synthetic jet for blowing and suction. Figure 24, below, shows that there are two pressure inlets and four pressure outlets on top with four walls. A diaphragm of length 0.05m acts as a velocity inlet by moving continuously. A structured mesh is preferred as mesh quality is the key for CFD solutions. Once the structure grid is produced, boundary conditions are assigned. Table 5 below shows the boundary conditions for the synthetic jet in air and water and the equations.

Table 5: Boundary condition for synthetic jet in air and water

S/No	Boundary conditions	Number of connectors
1	Synthetic jet	1
2	Pressure inlet	2
3	Pressure outlet	4
4	Wall	4
5	symmetry	4

The No slip condition of the wall except diaphragm is written as:

$$u(x, y) = 0 \quad (4)$$

$$v(x, y) = 0 \quad (5)$$

The velocity inlet condition at the oscillating diaphragm is written as:

$$u(x, y = \text{const}, t) = 0 \quad (6)$$

$$v(x, y = \text{const}, t) = v_j \sin(\omega t) \quad (7)$$

Where v_j is the velocity amplitude of the diaphragm.

In this equation, ω is related to the frequency, f by the relation:

$$\omega = 2\pi f \quad (8)$$

- Velocity inlet is the synthetic jet which oscillates at frequency of 700 HZ and amplitude of 0.05m/s.
- Pressure outlet boundary condition is used to define the static pressure at flow outlets.
- Wall boundary conditions are used to bound fluid and solid regions .In viscous flow no slip boundary condition is enforced at walls by default.
- ANSYS Fluent Solver is selected then the file is exported in to fluent.

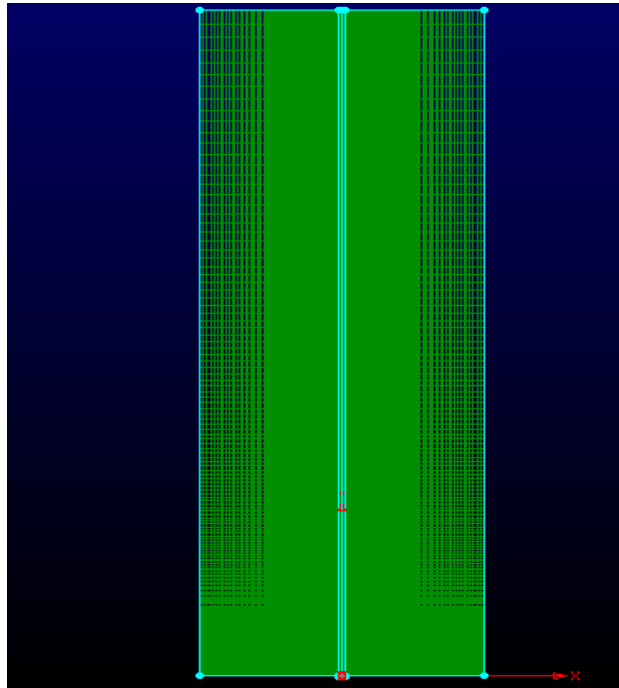


Figure 24: Grid generated for the synthetic jet in air

Once the mesh is generated and all conditions is given it is saved as .CAE file then open the .CAE file and select 2D and double precision and display mesh once it is done fluent allows us to change the mesh scale option where we can change mesh scale according to our need the mesh check as to be done. And in initial condition pressure based solver is selected followed by transient and viscous laminar for simulation, UDF is interpreted for sinusoidal velocity of diaphragm and air is selected in material Reference values are computed from the velocity inlet Standard pressure and first order upwind momentum spatial discretization is chosen as solution methods Relaxation factors are set at default values, Then the solution is initialized Time step size (S) and the number of time steps are chosen depending on frequency of the periodic motion. Then solution is calculated. Once

the solution is converged post results were analyzed in TECPLOT. The pressure Vorticity and velocity contour plots were obtained and velocity stream lines plotted.

3.4.2 Results

Before studying the influence of synthetic jets on vortices in a cavity, synthetic jet actuation is examined in a quiescent flow. It helps verifying the assumed jet model and assessing the formulation of synthetic jets. The flow is assumed to be 2-dimensional, incompressible and laminar.

The boundary layer simulations are performed for amplitude of 0.05m/s. The frequency of the jet was set to be 700 Hz. Synthetic jets in a quiescent flow result from the interactions of a series of vortices that are created by periodically moving diaphragm. The exiting flow separates at both edges of the diaphragm and rolls into a pair of vortices.

A series of vortex pairs are symmetric with respect to the centerline of the jets. Typically the moving mechanisms of synthetic jet actuators, e.g. acoustic waves or the motion of the diaphragm or a piston, induce the pressure drop which alternates periodically across the exit slot.

Although the simulations in this research do not take into account the high-fidelity modeling for the synthetic jet actuation consisting of cavity, orifice and inner moving boundary, the result validate that the assumed velocity condition contains the essential conditions of synthetic jets.

The pressure contour plots and the velocity vector plots for both suction and blowing have been shown below.

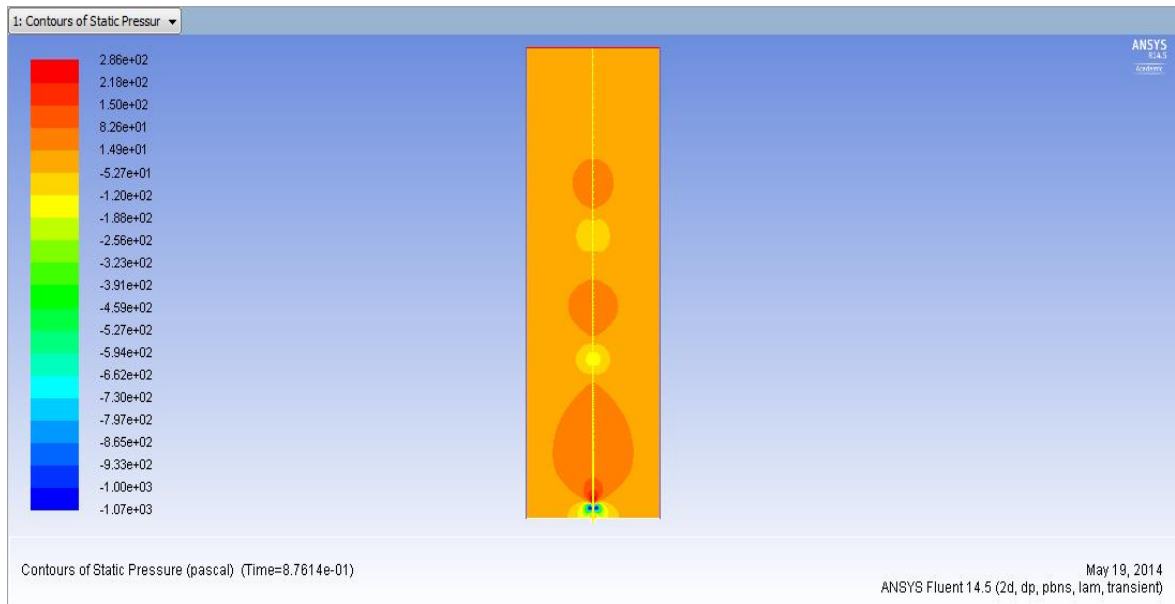


Figure 25: Pressure at Peak suction of synthetic jet

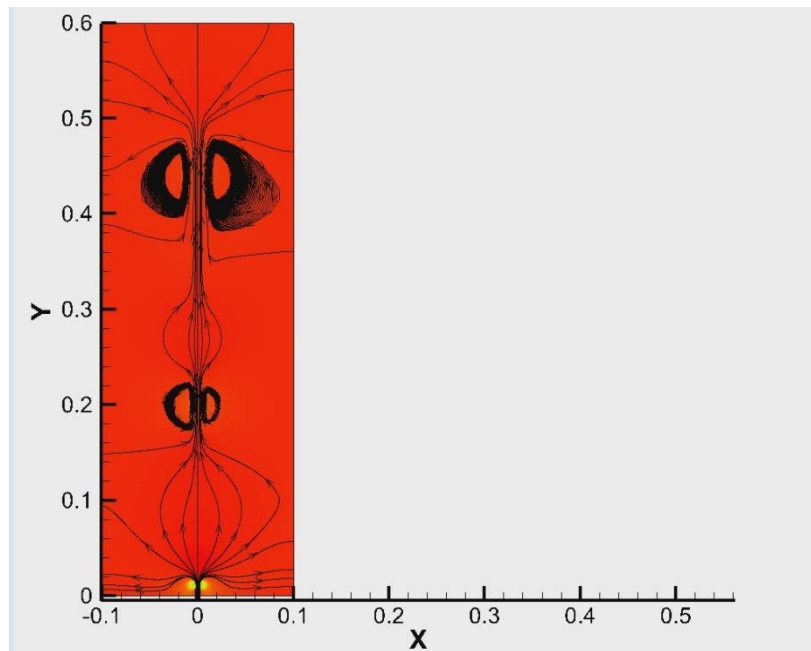


Figure 26: Pressure at Peak blowing of synthetic jet

3.5 Synthetic Jet in a Cavity with Two Pressure Outlets

This section covers the research for a synthetic jet in a cavity, where the interaction of a modeled synthetic jet is investigated numerically using incompressible Navier-stokes solver. The diaphragm is attached beneath the square cavity and the jet flow is observed. The simulation shows some interesting flow physics associated with vortex dynamics of the jet and also shows the behavior of vortices in the cavity. The jet is actuated at a frequency of 10Hz for all the cases with velocity amplitude of 0.05m/s, giving a Reynolds of 10^4 . Various results are extracted by varying the flow time.

3.5.1 Computational Grid and Methodology:

A grid is created using POINTWISE, where a $0.2\text{m}\times 0.2\text{m}$ cavity is created for blowing and suction, with a width of 0.02m and a depth of 0.002m. In Figure 27, it is shown that there are two pressure outlets on top along with four walls. The walls are given a no-slip condition and a diaphragm acts as a velocity inlet by oscillating. A structured mesh is generated and boundary conditions are assigned as show in Table 6.

Table 6: Boundary condition of synthetic jet in cavity

S/No	Boundary condition	Number of connectors
1	Synthetic jet	1
2	Pressure outlet	2
3	Wall	11

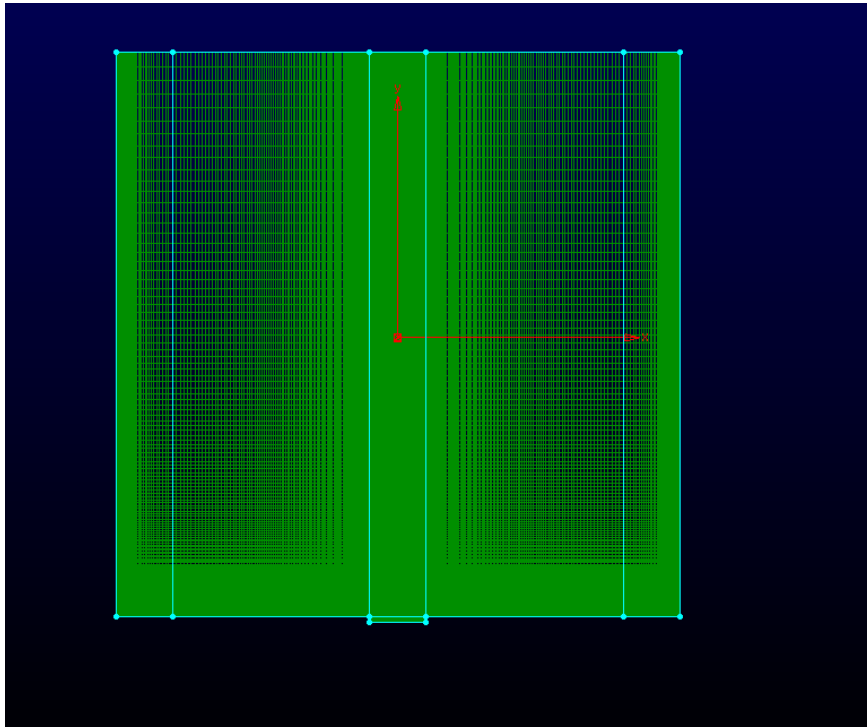


Figure 27: Grid generated for the synthetic jet with two pressure outlets

The same method is followed further for some cases by changing the amplitude and flow time. Table 7 shows the frequency of synthetic jet and amplitude of synthetic jet and flow time inside the cavity:

Table 7: Jet in cavity with different flow time and of Reynolds 10^4

Frequency of synthetic jet (Hz)	Amplitude of synthetic jet, V_j (m/s)	Flow time in cavity (s)
10	0.05	5
10	0.05	10
10	0.05	15
10	0.05	20

3.5.3 Results for cavity flow with symmetry

Synthetic jet in a cavity with two pressure outlets reveals interesting results, for flow time 5 seconds and 15 seconds the flow remains almost identical. With flow time 15 seconds two small vortices appear at bottom edges with four large vortices at the top. With flow time 10 seconds two large symmetric vortices are developed. Further with flow time 20 seconds the two large symmetric vortices as seen in 10 seconds flow time starts to diminish slowly.

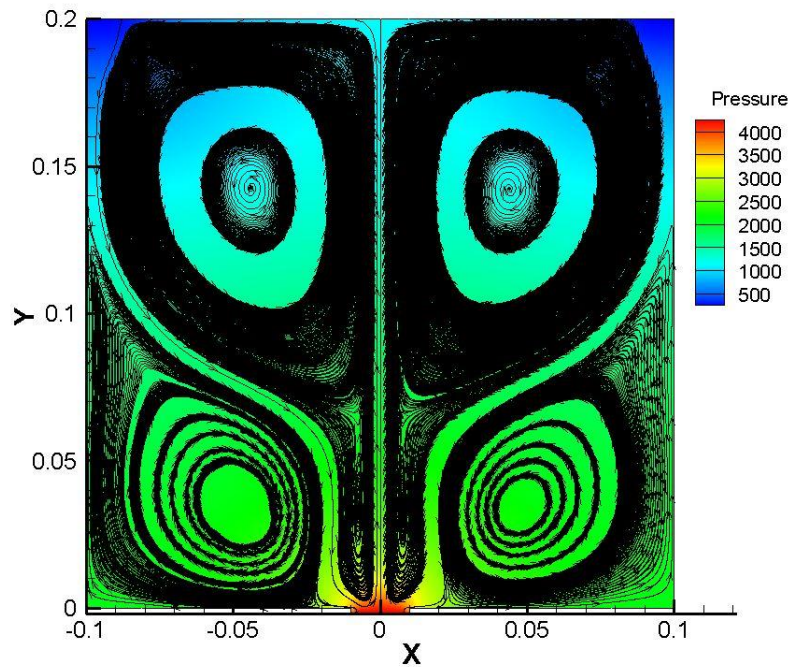


Figure 28: Symmetric Cavity flow at time= 5s

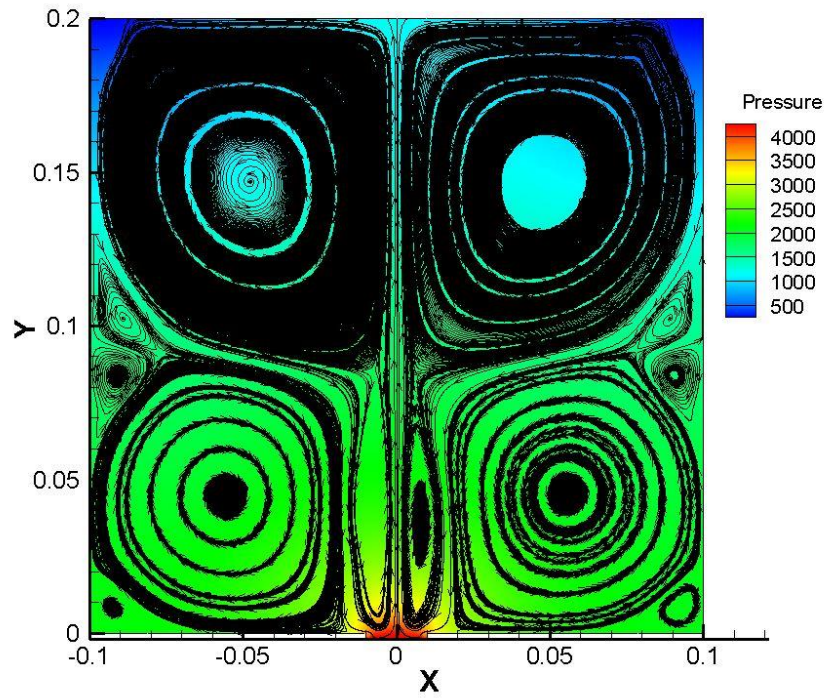


Figure 29: Symmetric Cavity flow at time= 10s

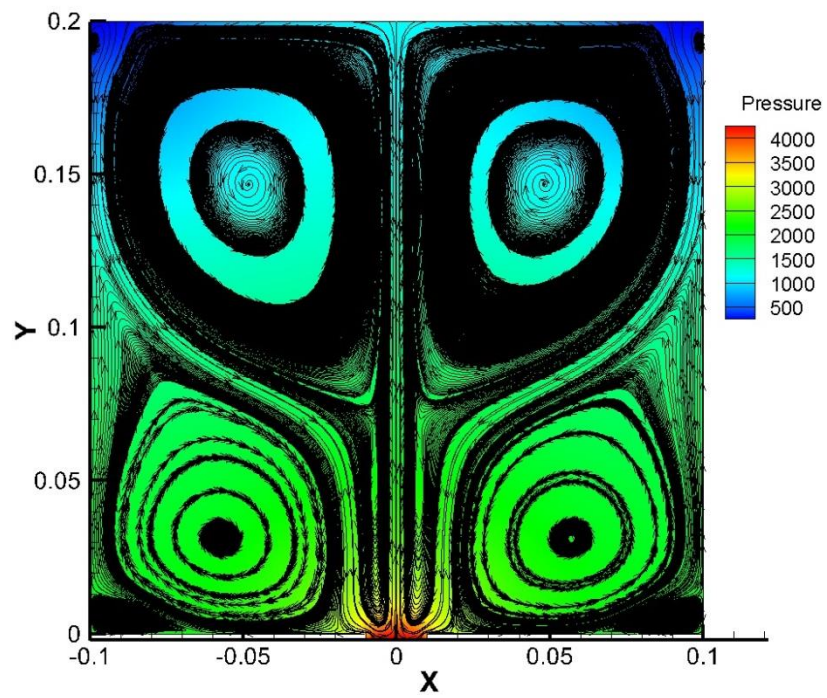


Figure 30: Symmetric Cavity flow at time= 15s

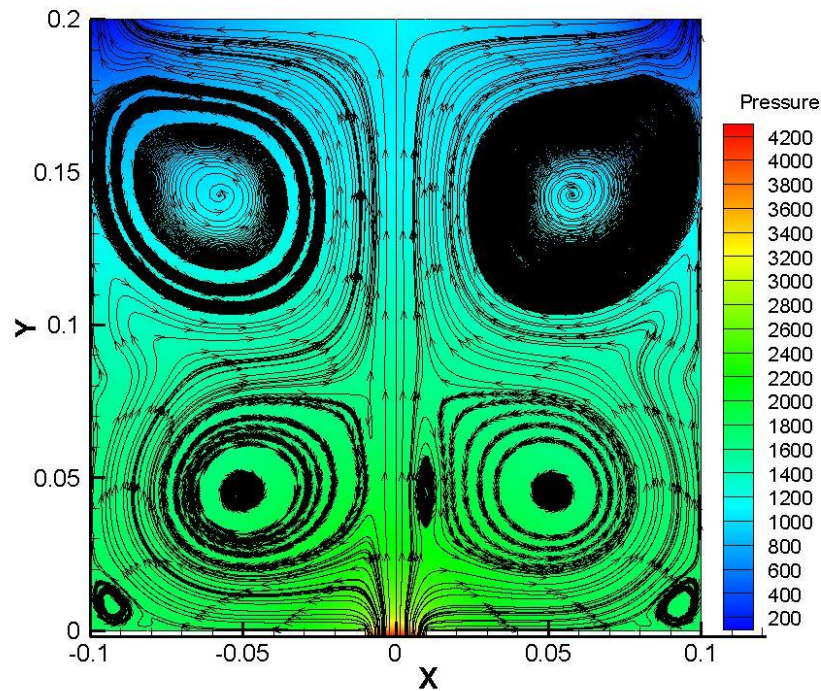


Figure 31: Symmetric Cavity flow with at time =20s

3.5.4 Results for Cavity Flow without Symmetry

In Figure 32 for frequency 10Hz velocity amplitude 0.05m/s and of flow time 5s it is seen that a just pair of two large vortices of same shape and two small of different shape appeared and started to rotate. the left vortex was rotating in anti-clock direction whereas right one on clock direction, in Figure 33 that due to flow time change two huge vortices which are same in 5s flow now changed their shape, in Figure 34 it is seen that the left vortex became larger and strong and right one is short and complex shape, in Figure 35 the large left vortex became stronger and with the formation of four more vortices structure became very complex.

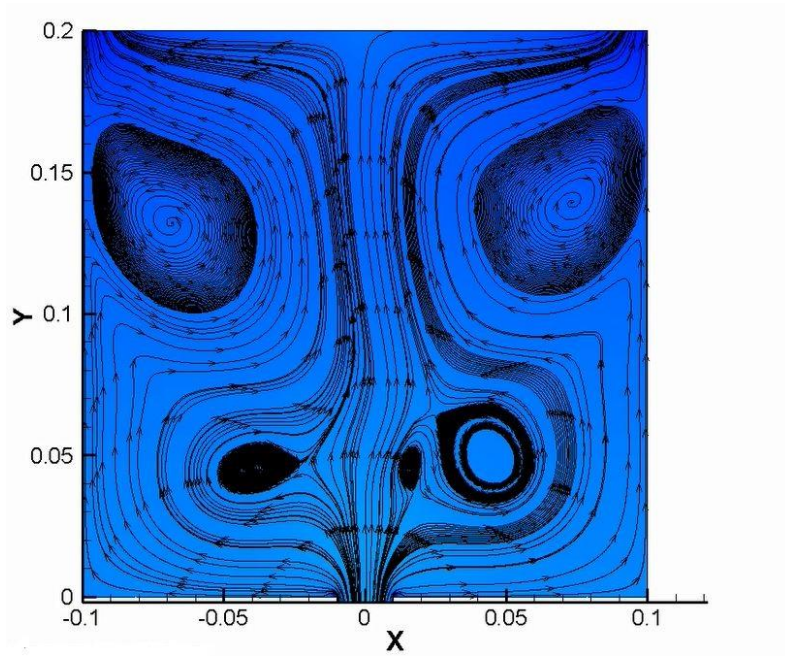


Figure 32: Cavity flow without symmetry at time = 5s

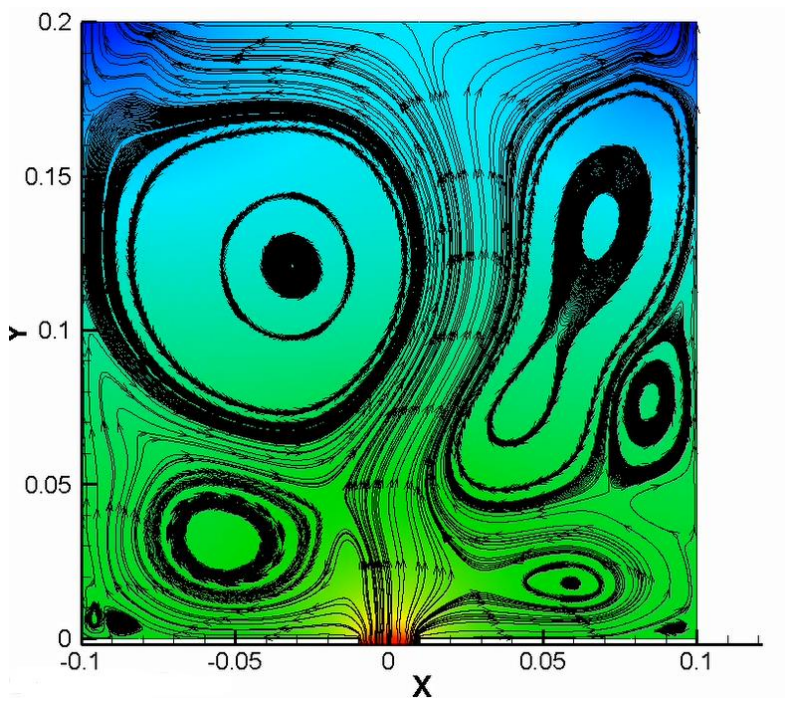


Figure 33: Cavity flow without symmetry at time = 10s

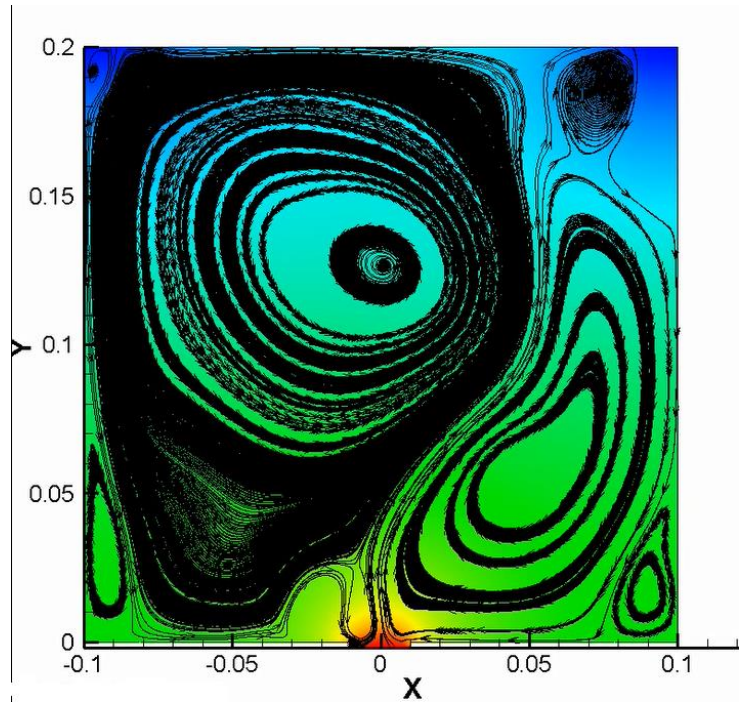


Figure 34: Cavity flow without symmetry at time= 15s

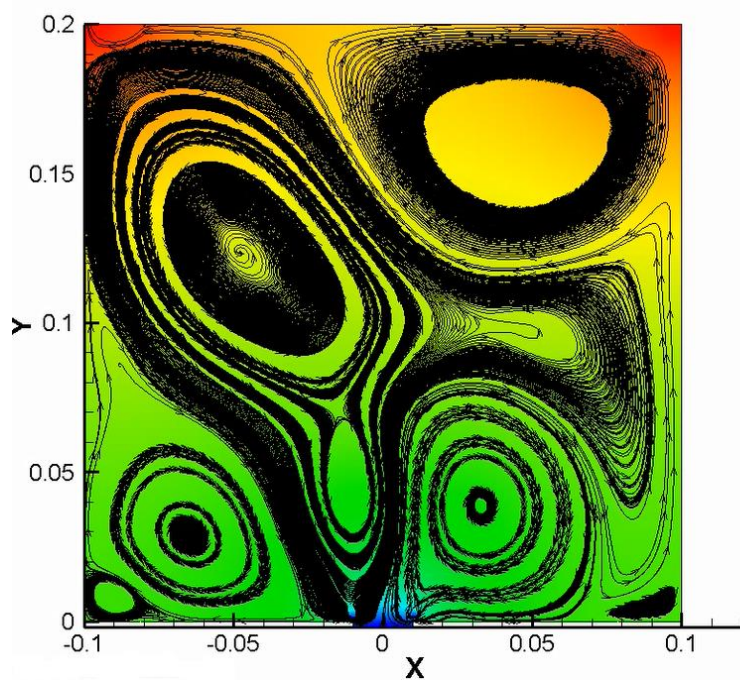


Figure 35: Cavity flow without symmetry at time= 20s

3.6 Comparison of the Cavity Flow Behavior for Symmetry and Non-symmetry

In Figure 36 a comparison of cavity with symmetry and non-symmetry is studied, for symmetry case a pair of identical vortices is observed, where for no- symmetry case a complex structure is observed with the formation of larger and smaller vortices of different shapes. So it has to be taken care of numerical errors while conducting experiment two get accurate results.

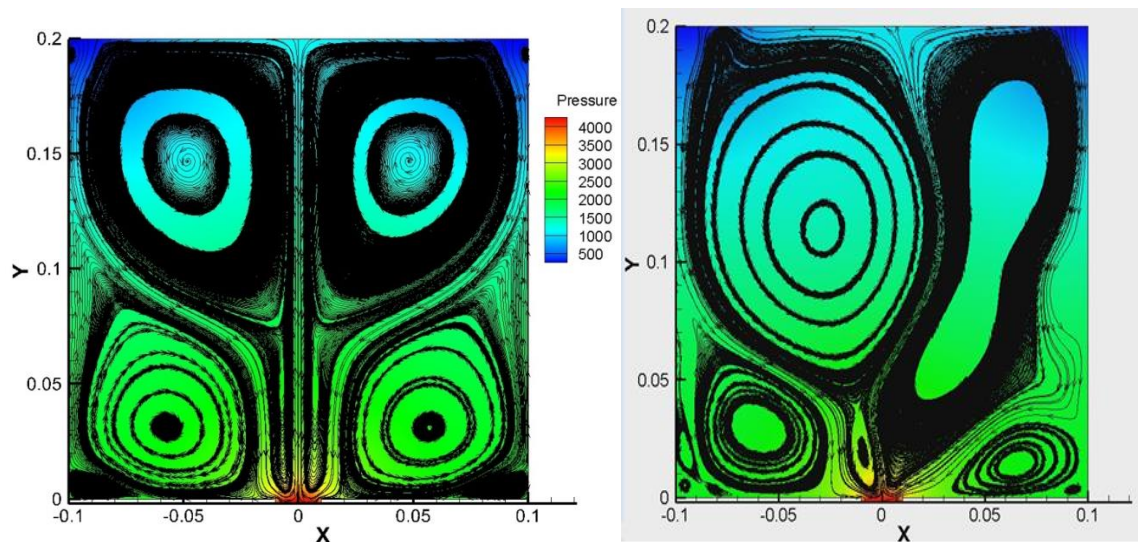


Figure 36: Comparison of the cavity flow behavior for symmetry and non-symmetry

3.7 Synthetic jet in velocity inlet and pressure outlet cavity

One of the challenges in this research is to avoid the vortices formed in the transient case. Based on previous research conducted in this area, it is seen that the synthetic jet is used to control the flow. Hence, the synthetic jets are placed in a cavity and observed to find the impact of a synthetic jet on a vortex flow.

3.7.1 Computational Grid and Geometry

The grid method remains same but the geometry is changed a square cavity of $0.2\text{m} \times 0.2\text{m}$ is designed in POINTWISE and with a velocity inlet and pressure outlet of 0.01m . A synthetic jet of length 0.02m and depth of 0.01m is located in different places as show in below geometry Figure 37 and Figure 38 and results are plotted.

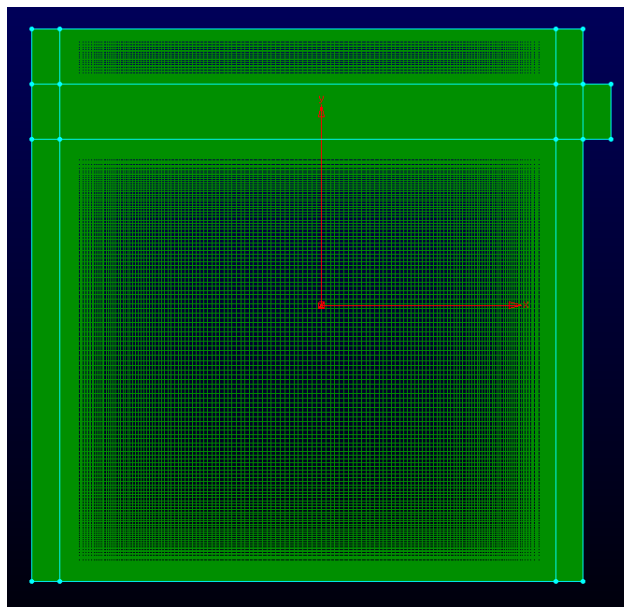


Figure 37: Grid generated for the synthetic jet located on the top right corner

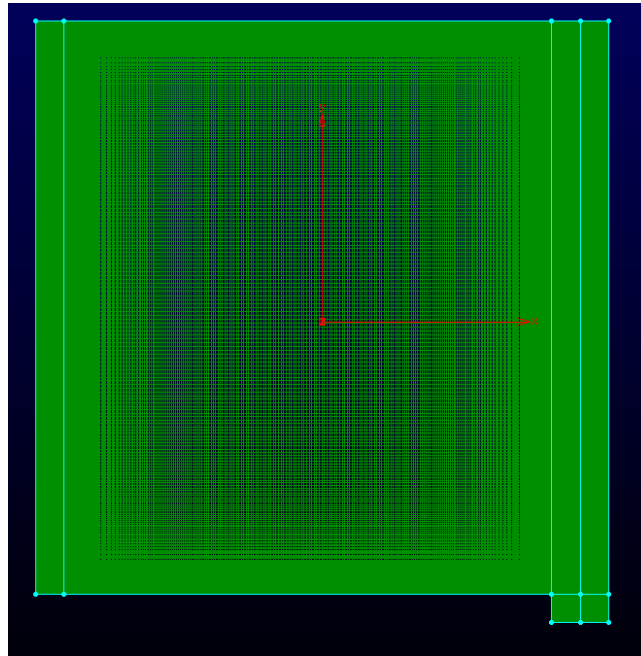


Figure 38: Grid generated for the synthetic jet located on the bottom right corner

3.7.2 Boundary Conditions

Table 8: Summary of the boundary conditions used for synthetic jet in square cavity

Boundary condition	Number of connectors
Velocity inlet	1
Pressure outlet	1
wall	11
Synthetic jet	1

The same method as of the synthetic jet in a cavity is followed. The velocity is given based on the Reynolds number.

3.7.3 Results

The simulation is carried out for various amplitudes. In Figure 39 it is seen that for an velocity amplitude of 0.002135m/s the vortex is pushed little towards pressure outlet by synthetic jet, and in Figure 40 for an velocity amplitude of 0.001708m/s two small vortices is appeared and for an velocity amplitude of 0.0014m/s the right one vortex is disappeared as shown in Figure 41. For velocity amplitudes of 0.004270m/s and 0.0085408m/s the vortex is pushed away to wards pressure outlet which is shown in Figure 42 and Figure 43.

Now in if Figure 44 it is seen that a simulation is done by placing synthetic at bottom it is observed for velocity amplitude of 0.00085408 m/s the big vortex became small with the formation of small vortex in left side of cavity

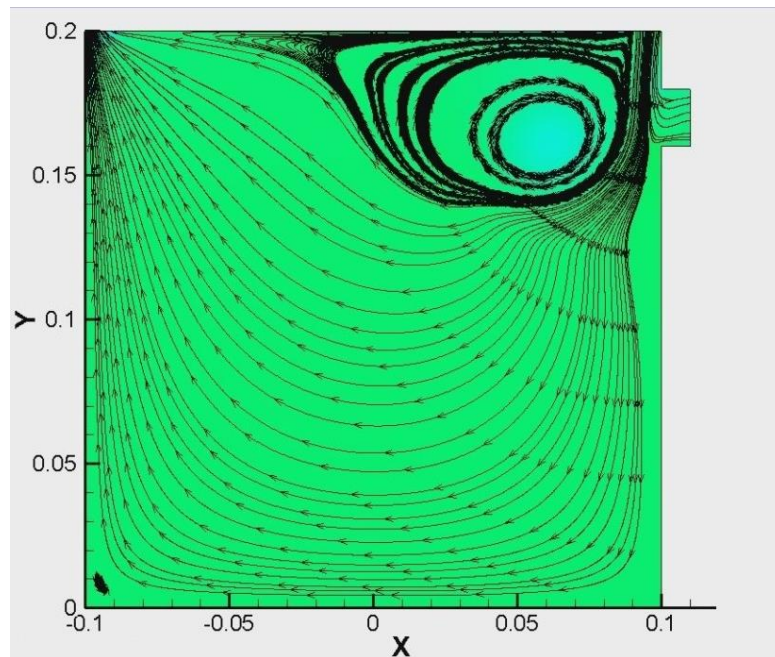


Figure 39: Velocity Amplitude $V_j = 0.002135$ m/s

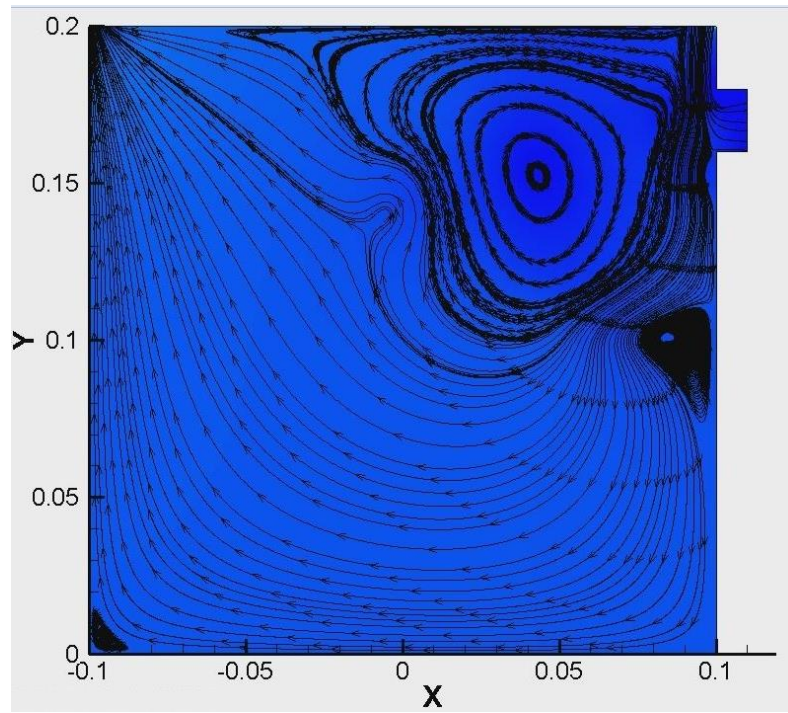


Figure 40: Velocity Amplitude $V_j = 0.001708$ m/s

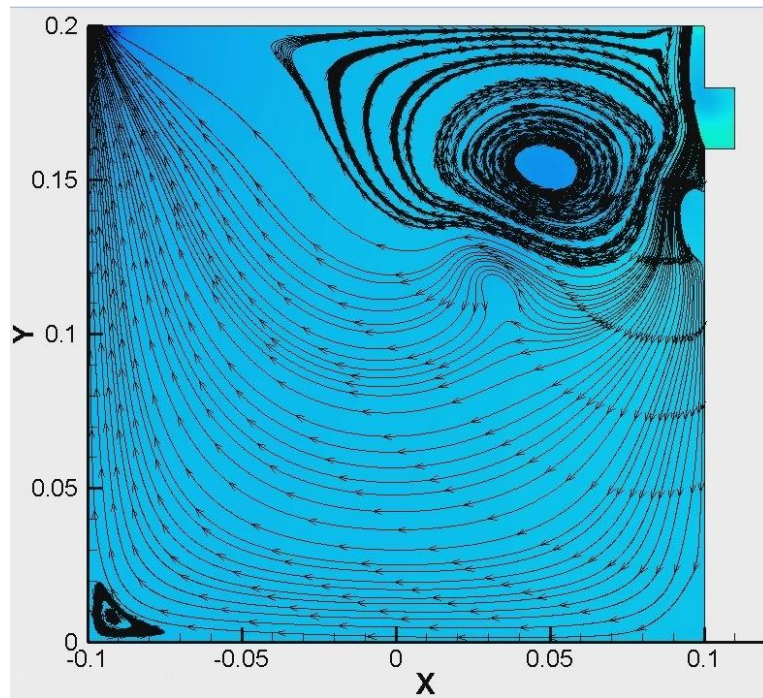


Figure 41: Velocity Amplitude $V_j = 0.0014$ m/s

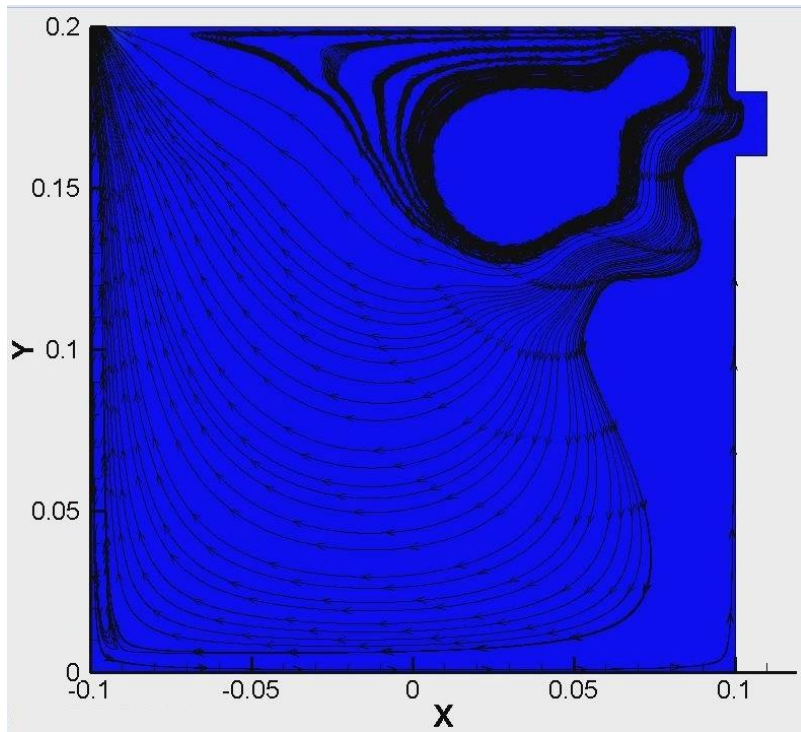


Figure 42: Velocity Amplitude $V_j = 0.004270$ m/s

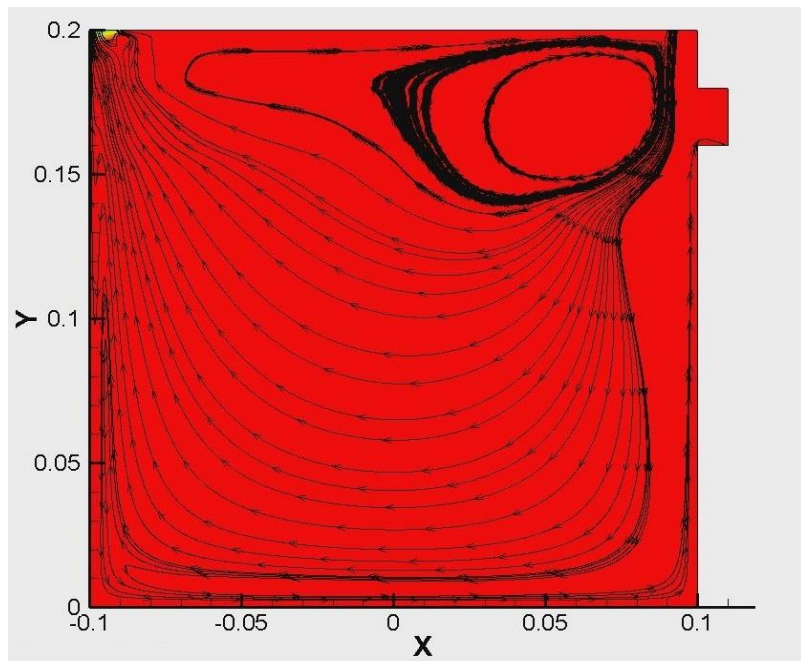


Figure 43: Velocity Amplitude $V_j = 0.0085408$ m/s

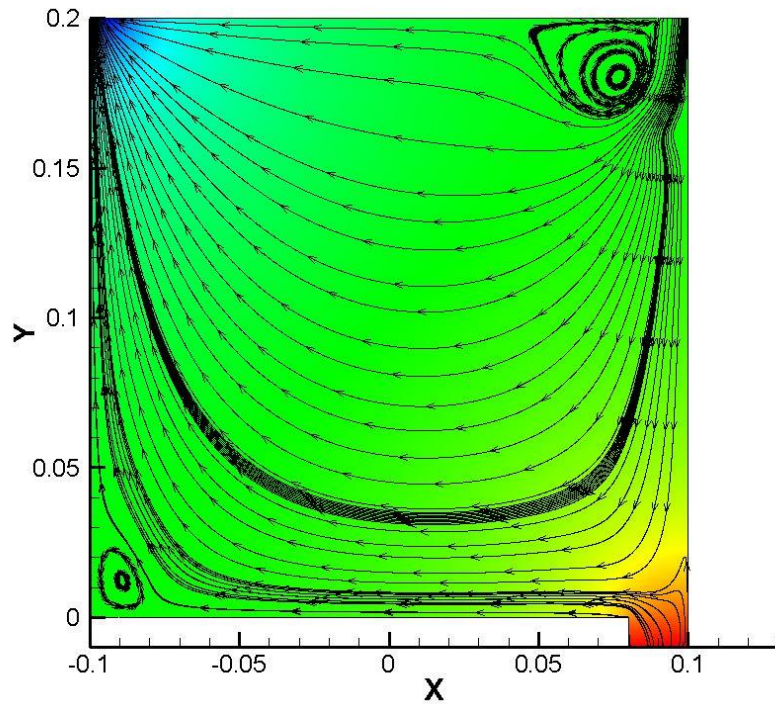


Figure 44: Velocity Amplitude $V_j=0.00085408$ m/s

4. CONCLUSION AND FUTURE WORK

The primary goal of this research is to study both the steady as well as the transient viscous, incompressible flow in a square cavity. By selecting the right time step size for the numerical integration of the unsteady Navier-Stokes equations, it was possible to obtain convergence to a steady state, which was found to be identical to the iterative solutions obtained by solving the steady N-S equations directly.

As a secondary goal some work was done on the problem of a synthetic jet in a cavity and its influence on the development of vortices inside the cavity. It is seen that there is some effect of the jet on the shape of the vortex, but it was not significant. For future work in the field of fluid flow separation control, it is recommended to place two or more synthetic jets, or by varying the orifice type of the synthetic jet or by changing the length and depth of the jet.

BIBLIOGRAPHY

Auerbach, D., "Experiments on the Trajectory and Circulation of the Starting Vortex". J. Fluid Mechanics Vol. 183, pp. 185-198, 1987.

Debiasi, M., "Experimental Exploration of Cavity Flow Physics", Retrieved from <http://www.marcodebiasi.net>, 2011.

Fernando, J. N., Kriegseis, J., and Rival, D. E., "Vortex Formation in Confined Rectangular-Cavity Flows." 31st AIAA Applied Aerodynamics Conference. June 2013.

Grottadaurea, M., and Rona, A., "Circular Cavity Flows", Department of Engineering, University of Leicester, Retrieved from <http://www.le.ac.uk/>, 2007.

Ahuja, K.K., and Chambers, W., "Prediction and Measurement of Flows over Cavities" - A survey ", AIAA 25th Aerospace Sciences Meeting I." January 1987.

Kral, L.D., "Active Flow Control Technology", ASME Fluids Engineering Division Technical Brief. 1999.

Gad-el-Hak, M., "Flow Control: Passive, Active and Reactive Flow Management". Cambridge University Press, 2000.

Isaev, S.A., 2-D laminar/turbulent driven square cavity flow. Retrieved from <http://www.cfd-online.com>, 2007

Isaev, S.A., Baranov, P.A., Kudryavtsev, N.A., Lysenko, D.A., and Usachov, A.E., "Simulation of A Circulation Laminar Flow Around A Square Cavity With A Mobile Boundary at High Reynolds Numbers With The Use Of Vp2/3 And The Fluent Package." Journal of Engineering Physics and Thermophysics, Vol. 78, No. 4, 2005.

Isaev, S.A., Baranov, P.A., Kudryavtsev, N.A., Lysenko, D.A., and Usachov, A.E., "Complex Analysis of turbulence models, algorithms, and grid structures at the computation of recirculating flow in a cavity by means of VP2/3 and FLUENT packages. Part 1. Scheme factors influence." Thermo physics and Aeromechanics, Vol. 12, No. 4, 2005.

Isaev, S.A., Baranov, P.A., Kudryavtsev, N.A., Lysenko, D.A., and Usachov, A.E., "Complex Analysis of turbulence models, algorithms, and grid structures at the computation of recirculating flow in a cavity by means of VP2/3 and FLUENT packages. Part 2. Estimation of models adequacy." Thermo physics and Aeromechanics, Vol 13, No 1, 2006.

Ghia, U., Ghia, K.N., and Shin, C.T., “High-Re Solutions for Incompressible Flow Using the Navier-Stokes Equations and Multigrid Method”, *Journal of computational physics* 48, Pages 387-411, January 15, 1982.

Barbagallo, A., Sippi, D., Jacqin, L., “Control of an Incompressible Cavity flow using a Reduced model based on Global modes”, 5th AIAA Theoretical fluid mechanics conference, 2008.

Donovan, F., “A Numerical Solution of Unsteady flow in a Two Dimensional Square Cavity”, *AIAA Journal*, Vol. 8, No 3, 1970.

Baurle, R.A., Tam, C.J., and Dasgupta, S., “Analysis of Unsteady Cavity flows for Scramjet Applications”, 36th AIAA/ASME/SAE/ASEE Joint Propulsion Conference, 2000.

Rona, A., and Dieudonne, W., “Unsteady Laminar and Turbulent Cavity flows models by Second order upwind methods”, 37th Aerospace Science Meeting and Exhibit, 1999.

Borland, C.J., “Numerical Prediction of the Unsteady flow field in open Cavity”, AIAA 10th Fluid and Plasma Dynamics Conference, 1977.

Takakura, Y., Higashino, F., Yoshizawa, T., “Numerical study on Unsteady Supersonic Cavity flows”, AIAA Fluid Dynamics Conference, 1996.

Verdugo, F.R., Guittion, A., Camussi, R., “Experimental Investigation of a Cylinder Cavity in a Low Mach Number flow”, *Journal of fluid and structures*, 2012.

Wang, G., Zhang, Z., Liu, M., “Control of Vorticity of flow over a Cavity with the Aid of Large Eddy Simulation”, *Procedia Engineering Journal*, Elsevier, Vol. 15, pp. 4228-4235, 2011.

APPENDIX

The User Defined function for transient velocity

inlet_velocity_profile.c

UDF for specifying a transient velocity profile boundary condition

```
#include "udf.h"

DEFINE_PROFILE(inlet_velocity, thread, position)
{
    face_t f;

    real t = CURRENT_TIME;

    begin_f_loop(f, thread)
    {
        F_PROFILE(f, thread, position) =  $V_j * \sin(\omega * t)$ ;
    }

    end_f_loop(f, thread)
```